Journal of Paleontology, 88(6), 2014, p. 1120–1138

0022-3360/14/0088-1120$03.00
DOI: 10.1666/13-142

SIZE, SHAPE, AND SYSTEMATICS OF THE SILURIAN TRILOBITE *AULACOPLEURA KONINCKII*

PAUL S. HONG,[1] NIGEL C. HUGHES,[2] AND H. DAVID SHEETS[3]

[1]School of Earth and Environmental Sciences, Seoul National University, Seoul 151–747, Korea, <hongps@hotmail.com>;
[2]Department of Earth Sciences, University of California, Riverside, CA 92521, USA, <nigel.hughes@ucr.edu>; and
[3]Department of Physics, Canisius College, 2001 Main St, Buffalo, NY 14208, USA, <sheets@canisius.edu>

ABSTRACT—A new dataset of the highest quality specimens of fully articulated, juvenile and mature exoskeletons of the Czech middle Silurian trilobite *Aulacopleura koninckii* offers improved resolution of original morphology by all measures considered. The degree of variation in both size and shape among later meraspid instars was constant, and suggesting targeted growth in both attributes. Size-related changes in the shape of the dorsal exoskeleton and of the segment-invariant cephalon were detected in the meraspid stage, but in the holaspid phase marked allometry was detected only in the trunk region, with the pygidium showing notable expansion in relative size. Meraspid cranidial allometry was subtle, with significant changes in instar form detectable only after several molts. This trilobite developed gradually throughout meraspid and holaspid ontogeny, with the synchronous cessation of trunk segment appearance and release at the onset of the holaspid phase. Precise development of shape and size occurs in the context of marked variability in the number of trunk segments at maturity, illustrating complex patterns of character variation within a species. A new systematic description establishes the synonymy of several subspecies with *A. koninckii*.

INTRODUCTION

THIS STUDY concerns the development of shape and size in a species that has provided important glimpses into the factors controlling developmental regulation in trilobites, the middle Silurian trilobite *Aulacopleura koninckii*. Large numbers of articulated exoskeletons covering a broad span of juvenile and mature ontogeny occur in a thin interval of siltstone on Na Černidlech Hill near Loděnice in the Czech Republic (Hughes et al., 2014). Mature specimens within this assemblage show the greatest degree of intraspecific variation in thoracic segment number known in any hemianamorphically-developing trilobite (Hughes et al., 1999; Hughes et al., 2006), and the presence of such variability in a Silurian trilobite is remarkable because variation in thoracic segment numbers is generally rare among post-Cambrian trilobite species (Hughes et al., 1999). Of particular interest is to learn how the marked degree of variation in thoracic segment number seen in *A. koninckii* relates to other aspects of the development of this animal, and what insights might this variation provide into the microevolutionary basis of the macroevolutionary changes in the evolutionary history of these early arthropods. This study documents the construction of the new dataset, evaluates its quality, and uses it to explore variation in the size and shape of the major exoskeletal components of *A. koninckii* in novel ways. This information is then integrated into an updated systematic description of this taxon.

GEOLOGICAL SETTING

All the material considered in the quantitative analysis presented below came from a 1.4 m interval of the Homerian *Aulacopleura* shales at "Barrande's pits" on Na Černidlech Hill that likely accumulated over an interval spanning a few thousand years (Hughes et al., 1999; Hughes et al., 2014) on the flanks of the the Perunican microcontinent (Štorch, 2006; Fatka and Mergl, 2009). *Aulacopleura koninckii* occurs in large numbers as articulated, partially articulated, and disarticulated specimens on multiple bedding planes within this interval. Occasional enrolled specimens suggest that individual surfaces were buried by obrution, but the degree of disarticulation present on bedding plane collections suggests that all surfaces are time-averaged to some extent. The assemblage is an example of a Type I trilobite lagerstätte in which large numbers of partially articulated specimens are preserved in situ (Brett et al., 2012; Hughes et al., 2014). Prone specimens apparently include both carcasses and intact exuviae, and mean specimen size can vary markedly between individual bedding plane assemblages. On some bed surfaces, *A. koninckii* is accompanied by a diverse range of Silurian skeletonized benthos, but others are monospecific assemblages of *A. koninckii*. No morphological variations were observed that could localize individuals from one bedding plane from those from any other bedding plane.

PRIOR RESEARCH ON THE DEVELOPMENT OF *A. KONINCKII*

Barrande (1852) described the meraspid ontogeny of *A. koninckii*, documenting the sequential addition of segments, and also noted that large individuals from Na Černidlech displayed between 18 and 22 thoracic segments. Multivariate analysis of various linear dimensions of 86 specimens (Hughes and Chapman, 1995) detected no correlation between the number of segments in the thorax and in the meraspid or holaspid pygidium. Accordingly, variation in thoracic segment numbers was not evidently compensated for, or explained by, variation in the number of pygidial segments.

A Procrustes-based geometric analysis compared morphological variability among holaspid *A. koninckii* with that of the holaspids of six other trilobite species present in 1.4 m interval (Hughes et al., 1999) each of which were invariant in the holaspid number of thoracic segments (Hughes et al., 1999; Hughes and Chapman, 2001). The comparable levels of shape variation in each contrasted with the variability in thoracic segment numbers seen in mature *A. koninckii* and suggested a degree of compensation between the number of thoracic segments and the sizes of individual segments in that species.

Analysis of 391 well-preserved specimens, ranging from forms 1.5 mm long with five thoracic segments to large

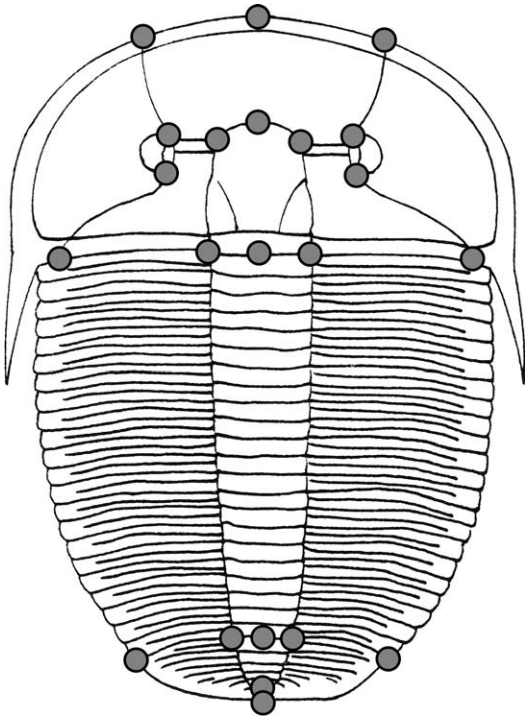

FIGURE 1—Gray dots show position of fifteen cranidial landmarks and seven pygidial landmarks considered in this analysis on the dorsal exoskeleton of *Aulacopleura koninckii* (modified from Hughes and Chapman, 1995, fig. 3).

holaspids over 24 mm long (Fusco et al., 2004) showed that *A. koninckii*'s meraspid growth rate between stages (=intermolt phases=instars) was extremely constant from meraspid stages 5–17. It conformed to Dyar's rule, a geometric progression of size increase typical of the development of many arthropods, but not previously recorded in trilobites over an extended set of molts. The analysis also showed that the degree of size variance within stages remained constant during growth. This indicated that size increase in *A. koninckii* was targeted during this portion of ontogeny, rather than showing an expansion of variance that commonly accompanies growth.

The determination of thoracic segment number at the transition into the mature growth phase was tested by looking at the size-frequency distributions of individuals at the transition from meraspid to holaspid growth, and by the growth of the pygidium (Fusco et al., 2004). Results from both analyses supported the idea that the number of mature thoracic segments was determined precociously and, therefore, independently from meraspid growth. The sample composed of five distinct cohorts that were apparently morphologically identical during meraspid growth. Membership of a particular cohort could be under either hereditary (e.g., genetic) or environmental influence.

Hammer and Harper (2006, p. 148) using a dataset modified from that of Hughes and Chapman (1995) discerned several patterns of size-related shape change and also detected an element of shape variation that was induced by shear stress, which they suggested accounted for a small proportion of the total shape variance (see also Hughes et al., 2014).

Fusco et al. (2014) demonstrated a growth gradient among late meraspid trunk segments and showed the presence of a regional control that was stable across all developmental stages investigated.

To date, analyses of the meraspid growth of *A. koninckii* have focused on information about instar size attributes. In this analysis, we present an investigation of the development of both size and shape. To do this, we have constructed a new and highly selective dataset of specimens that limits taphonomically-induced morphological variance to a minimum. We describe the meraspid and holaspid ontogeny of *A. koninckii* with respect to growth allometry and assess whether any marked change in allometric trajectory coincides with changes in other aspects of development. We also assess the instar-related pattern of growth rate in size and shape during meraspid ontogeny.

THE SAMPLE

All specimens were completely articulated dorsal exoskeletons preserved in prone posture for which a set of 22 morphological landmarks, 15 in the cranidium and seven in the pygidium (Fig. 1), were available (see online Supplemental Data File 1). Specimens were coated with ammonium chloride or magnesium oxide sublimate prior to digital photography. Given preservation in shale, with inevitable compaction associated (Hughes, 1999; Hammer and Harper, 2006, p. 153; Hughes et al., 2014), a simple estimate of measurement error was employed. The standard deviation of cranidial length estimates were less than 0.026 millimeters in all cases, and the error amounted to less than 0.6% of each linear measurement (online Supplemental Data File 1). This is less than the 0.8% size error estimate recorded in the Fusco et al. (2004) study. Shape variance, not previously assessed for error in *A. koninckii*, was estimated by repeated digitization of 15 cranidial landmarks for each of the five specimens, and variance values, calculated as the average Procrustes distance from the mean form, which was about 0.0005 in all cases. (All statistical analysis conducted in the paper using programs within the Integrated Morphometrics Package written by H.D.S., see online Supplemental Data File 2 for details of programs used). This value of shape variance is an order of magnitude lower than the variance from mean shape for members of the same meraspid segment number cohort (see analyses below), suggesting that measurement error accounts for small proportion of the observed shape variance. Most specimens are internal molds, and sclerite thickness was not accounted for in our measurements. Taphonomically induced limitations constrain our ability to discern the finest scale patterns of biological variation evident in some trilobites preserved in silica or phosphate (Webster, 2011), but is unavoidable if large numbers of articulated specimens are to be examined.

We have attempted to limit the effects of taphonomy by restricting our database to only those specimens of the highest preservational quality available. Analyses previously conducted on the original, less restrictive, dataset were repeated in order to determine whether patterns seen in earlier work remain robustly supported. Where appropriate we have also considered the possible influence of taphonomy on results.

The new dataset included individuals selected from the over 10,000 specimens inspected in six major collections (Online Supplemental Data File 3). Only those specimens that were complete for all landmarks showed no evidence of "telescoping" of the thorax or any other evident shape deformation were included, and these 352 specimens constituted approximately 4% of prone complete dorsal exoskeletons of *A. koninckii* available (Online Supplemental Data File 3). To explore whether we could distinguish different patterns of variation within this sample based on preservational differences we assigned each of these specimens to one of two taphonomic grades based on their preservational quality, with near "perfect" specimens assigned to taphonomic grade 1 material (N=44), and slightly less well-preserved specimens assigned to grade 2

https://doi.org/10.1666/13-142 Published online by Cambridge University Press

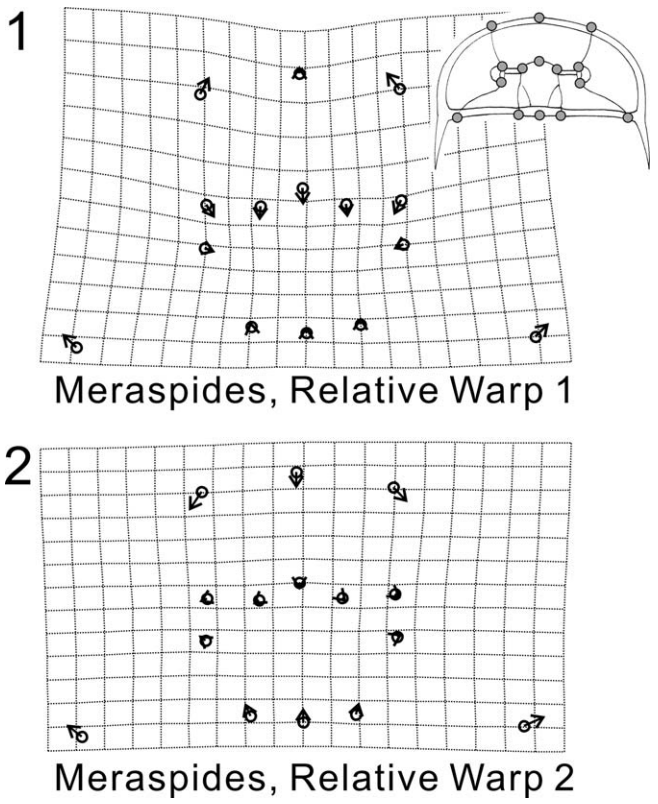

FIGURE 2—Thin-plate spline deformation grid of relative warps for the 15 cranidial landmarks of all meraspid and holaspid specimens of *A. koninckii* (*N*=352): *1*, shape variation related to Relative Warp (RW) 1 (24.80% of total variance, depicting size of the pleural region relative to the glabella and the palpebral lobes); *2*, shape variation related to RW2 (22.23% of total variance, depicting an axis of cranidial expansion in transverse direction), direction of shape variations inversed in order to match those seen in majority of other landmark configurations and other subgroups of the sample.

(*N*=308) (see Online Supplemental Data File 4 for details and statistical comparisions).

Comparisons of variance in both size and shape between specimens assigned to Grade 1 and Grade 2 show that although Grade 1 specimens do show lower variance than Grade 2, the differences are not statistically significant for any meraspid instar (Online Supplemental Data File 4). Accordingly, all 352 specimens were subsequently treated as a single sample for statistical analysis. We conclude that our sample represents the highest quality of preservation of *A. koninckii* from Na Černidlech currently available, but that is not entirely free from taphonomic influence, as discussed below.

The new dataset represents the growth history of multiple consecutive instars of *A. koninckii*, from meraspid degree 4 to later holaspid ontogenetic stages, but from meraspid degree 9 onward the sample size is over 10 specimens per instar, so analyses of size and shape concentrated on meraspid stages 9–17. The largest holaspid exoskeleton is 28.81 mm long. Out of the 352 specimens, 148 specimens (42.0%) are definitive meraspids ranging between degree 4 to degree 17. Other specimens are mostly holaspid or later stage meraspids of the segment-rich morpohtypes (Online Supplemental Data File 5).

A comparison of the new dataset with that used in the Fusco et al. (2004) study, which is of comparable size to the new one, shows that the variance of the logarithm of the cranidial centroid size (ln CCS) (Online Supplemental Data File 6) is notably lower. Although no significant differences between the variance estimates for each meraspid morph was detected at the 95% confidence level (two-tailed F-test for individual meraspid stage comparison: p=0.813∼0.089), the shortest unbiased confidence intervals at 95% level and variance values are consistently lower in the new dataset. The variance in shape also displayed reduced values in the new dataset, with variance values consistently lower than the previous dataset, and the 95% confidence intervals calculated based using 1600 bootstrap resamples were almost significantly different between the two datasets (Online Supplemental Data File 6).

These results suggest that the new dataset shows markedly less shape and size variance within individual morphs than the old one. This we interpret to be the result of the more stringent criteria applied to specimen selection and an improved protocol for digitization that involved constructing a line down the sagittal axis of the trilobite that helped pinpoint landmark positions, and possibly also improved equipment. It suggests that the variation that we have now captured better approximates the original variation among the living animals.

As noted above, Hammer and Harper (2006) detected a component of variance in the positions of landmarks to indicate the action of shear stress (6.2% of overall variance, associated with principal component [PC] 2, in their study). In our analysis, the third PC of a principal component analysis (PCA) of the landmark displacement from the average shape for entire dataset revealed a pattern consistent with shear stress, and accounted for 4.8% of the variation. Both results suggest that simple shear accounts for a small proportion of total variance in the new sample, but has not been entirely excluded even in this highly selective dataset in which all specimens showing obvious shear were excluded (see also Hughes et al., 2014).

QUANTITATIVE DESCRIPTION OF ONTOGENETIC SHAPE CHANGE

Ontogenetic shape changes during meraspid and holaspid growth.—Such changes were achieved in several ways: within individual skeletal components, via the addition of new skeletal components (e.g., trunk segments), and through changes in the relative sizes of different skeletal components. Cranidal and holaspid pygidial changes are discussed in this section, followed by a consideration of the ontogeny of overall proportions. Details of the growth of individual trunk segments are given in Fusco et al. (2014).

Cranidial shape changes.—Analysis of cranidial shape change was based on 15 cranidial landmarks (Fig. 1) using geometric morphometric methods (Zelditch et al., 2004). A PCA of the partial warp scores (derived from the thin-plate spline analysis of Procrustes aligned landmarks based on the mean shape of the whole) shows that almost half of the total variance is captured by the first two principal components: Relative Warp (RW) 1 and RW2 respectively each explain 24.8% and 22.2% of the total shape variance. Other RWs each account for less than 10% of total variance and are not considered further (Online Supplemental Data File 7). RW2 apparently suggests an axis of cranidial expansion in the transverse direction, more pronounced in the marginal area such as the landmarks at the anterior and posterior ends of the facial sutures (Fig. 2). This pattern might be taphonomic in origin as it mimics that known to be associated with deformation in trilobites (Hughes and Jell, 1992). RW1 is a more complex pattern of shape change, and reflects expansion of the pleural regions of the cranidium relative to the glabella and palpebral lobes. Accordingly, the size of both the eye and the glabella declined relative to the overall size of the cranidium, with the intraocular distance also narrowing relatively as overall size increased (see below for results on regression of partial warp score against the natural log of the cephalic centroid size, ln CCS). These patterns accord with the analyses of Hammer and Harper (2006, p. 150), who reported positive allometry of the

https://doi.org/10.1666/13-142 Published online by Cambridge University Press

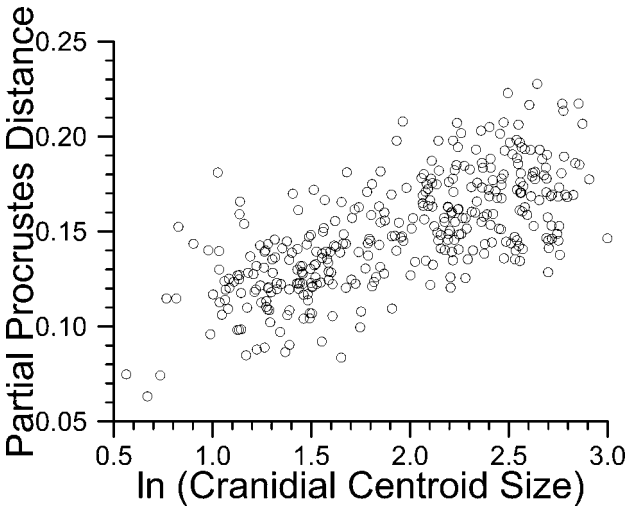

FIGURE 3—Partial Procrustes distance from the reference (mean shape of the smallest three specimens) of 15 cranidial landmarks for all specimens of holaspides and meraspides (N=352). Regression of partial Procrustes distance against logarithm of cranidial centroid size (ln CCS) is significant (slope=0.0365, $P<0.0001$, r=0.4808).

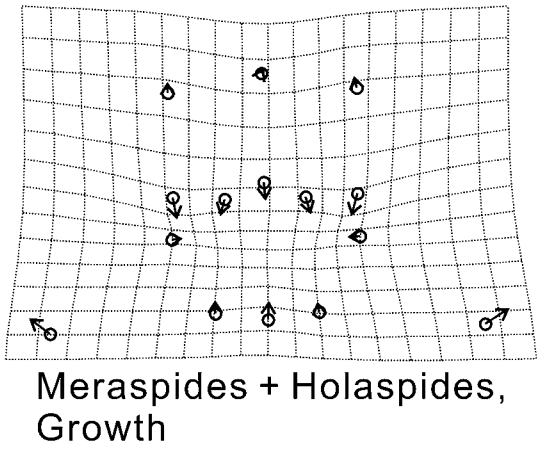

FIGURE 4—Thin-plate spline deformation grid of shape changes with growth for the 15 cranidial landmarks of all specimens of holaspides and meraspides (N=352). Partial warp scores are regressed in a multivariate regression against ln centroid size, and 14.7687% of total shape variance (based on summed squared residuals expressed in Procrustes units) is explained by the allometry ($P<0.000625$ from 1,600 bootstraps).

frontal area, but did not detect classic allometry in the palpebral lobe length. We concur with Hammer and Harper (2006, p. 150) that the palpebral lobe growth relationships may be complex, but suggest that any allometry between the eye and glabellar length is quite subtle. Plots of eye length relative to glabellar length through meraspid and holaspid ontogeny (Online Supplemental Data File 7) apparently suggest that the eye becomes slightly more prominent during meraspid ontogeny, but that its relative length wanes slightly during holaspid growth. However, statistical tests applied for the meraspid data and the five holaspid morphs separately (Online Supplemental Data File 7) failed to distinguish eye length changes from isometry.

In order to investigate whether any of these patterns represent ontogenetic change, the partial Procrustes distance of individual specimens from the mean of the smallest three specimens in the entire dataset was calculated (Fig. 3). A significant positive relationship exists between partial Procrustes distance and ln CCS (slope 0.0365, $P<0.0001$) and, when partial warp scores from mean shape were regressed against ln CCS, 14.8% of the total shape variance was explained by the growth allometry ($P<0.000625$ for 1,600 bootstraps). A deformation plot (Fig. 4) shows that the growth-related shape changes identified match those seen in RW1 (Fig. 2.1) and in a resistant fit theta-rho superimposition of cranidial landmarks of a different dataset (Hughes and Chapman, 1995, fig. 11). Accordingly, we consider these patterns to capture aspects of ontogenetic variation. Furthermore, the vector of the regression differs significantly, at the 95% confidence level, from isometry following 1600 bootstraps resamples (angle to isometry 109.4°, within sample angle 13.9°).

In order to determine if meraspid and holaspid growth phases differed in patterns of cranidial size-related shape, data from 148 specimens from meraspid degrees 4 through 17 were examined (Fig. 5, Online Supplemental Data File 8). RW1 (Fig. 5.1), which explains 26.35% of the total shape variance, appears to be very similar to RW2 (Fig. 2.2) derived from the combined meraspid and holaspid dataset. They both capture variation in the areal proportion of the pleural region relative to that of the glabella and the palpebral lobes. RW2 (Fig. 5.2) for meraspid degrees 4 through 17 explains 16.58% of the total variance, and likewise reflects growth-related shape variation seen in RW1 (Fig. 2.1) of the combined meraspid and holaspid dataset. Patterns derived from the combined meraspid and holaspid datasets and those derived from meraspid degrees 4 through 17 seem to be similar, with minor variations in the ordering of the relative warps but comparable patterns of shape variation. A positive relationship between the partial Procrustes distance and ln CCS (Fig. 6) is significant (slope 0.0314, $P<0.0001$), indicating significant meraspid cranidial allometry. Multivariate regression of the partial warp scores using mean shape as a reference against ln CCS is significant ($P<0.000625$ for 1,600 bootstraps) and explains 7.64% of total shape variance, and the vector of the regression coefficient differs significantly at 95% confidence level from isometry (angle to isometry 83.0°, within sample 30.6°). The pattern of shape change identified (Fig. 7) again mimics that seen in RW1 for the total sample (Fig. 2) and RW2 for the meraspid-only dataset. As the partial Procrustes distance displays a significantly positive relationship with ln CCS only when instars separated by four or more molts are compared (Online Supplemental Data File 8), the overall amount of ontogenetically related shape change in the meraspid cranidium is small. Nevertheless, this close similarity between RW1 for the total sample and RW2 for the meraspid-only dataset implies that the dominant pattern of shape change in the meraspid cranidium conforms to the ontogenetic trajectory. It was not possible to detect a stepped decline in the amount of shape change per meraspid instar (Online Supplemental Data File 8).

The PCA of partial warp scores suggest that similar types of shape variation seen in the meraspides are present in all holaspid morphs (Online Supplemental Data File 9). However, holaspides bearing 19 thoracic segments, the most numerous among the five holaspid segment number morphs, with ln CCS larger than 2.2 show no significant relationship between the partial Procrustes distance from the mean of the smallest three meraspids and ln CCS at the 95% confidence level (slope=0.0224, P-value=0.0543, r=0.2210) (Online Supplemental Data File 9). A similar result was obtained for all the other holaspid thoracic segment number groups, except for the morph 21, which did show a significant increase of partial Procrustes distance to ln CCS (Online Supplemental Data File 9). In addition, the partial warp scores for holaspid specimens of morph 19 are regressed in a multivariate regression against ln centroid size and suggest that size explains only 1.50% of the total variance, which is not

https://doi.org/10.1666/13-142 Published online by Cambridge University Press

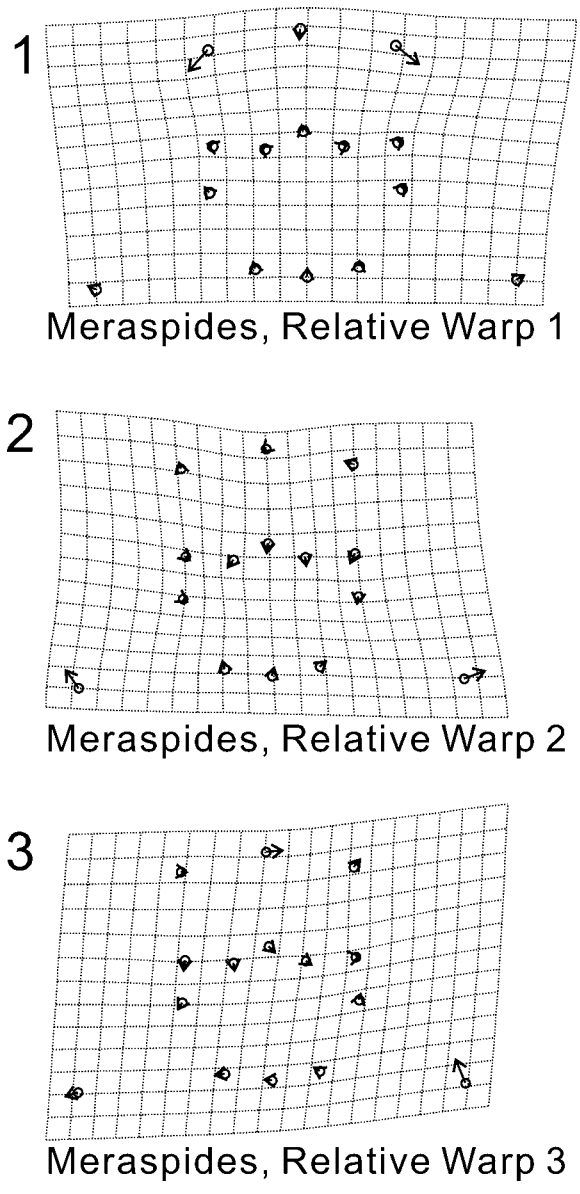

FIGURE 5—Thin-plate spline deformation grid of relative warps for the 15 cranidial landmarks of meraspides from meraspid degree 4 through 17 (N=148): *1*, shape variation related to RW1 (26.35% of total variance, depicting variations in the anterior width between the facial sutures); *2*, shape variation related to RW2 (16.58% of total variance, depicting size of the pleural region relative to the glabella and the palpebral lobes, direction inversed); *3*, shape variation related to RW3 (10.31% of total variance, depicting effects of shearing, direction inversed).

significant (P=0.578 for 1,600 bootstraps; Online Supplemental Data File 9; a similar result was obtained for the other morphs including holaspid specimens of morph 21: holaspid specimens of morph 18 were excluded from analysis due to small sample size). Accordingly, holaspid cranidial growth appears to be largely indistinguishable from isometry.

In order to explore whether there was any indication of a marked transition in cranidial growth pattern during observed ontogeny, we examined the relationships between partial warp scores and ln CCS. Results suggest that some partial warp scores have an apparently curvilinear relationship to size (Online Supplemental Data File 10), and thus do not provide clear indication of a sharp transition in cranidial growth pattern

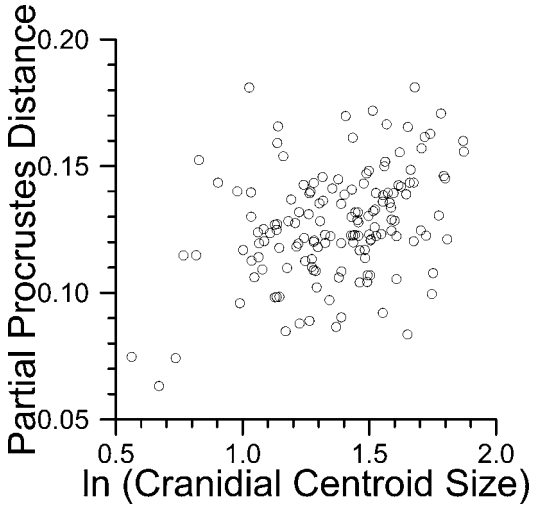

FIGURE 6—Partial Procrustes distance from the reference (mean shape of the smallest three specimens) of 15 cranidial landmarks for specimens of meraspides from meraspid degree 4 through 17 (N=148). Regression of partial Procrustes distance against logarithm of cranidial centroid size is significant (slope=0.0314, P<0.0001, r=0.1377).

associated with the meraspid/holaspid transition, although overall transition from allometry to isometry is noted above.

Pygidial shape changes.—Due to the changing complement of segments in the meraspid pygidium, it is problematic to treat the pygidium of different meraspid degrees as a homologous structure. For that reason our analysis is here restricted to holaspid pygidia, although it is acknowledged that the pygidia of each of the different morphs represent a different complement of trunk segments. For the holaspid pygidium, the PCA of the partial warp scores shows that more than half of the total shape variance is explained by RW1 (54.03%) in specimens with 19 thoracic segments (with its ln CCS values higher than 2.2). The RW2 and RW3 explained 14.78% and 13.20% of the variance respectively; other relative warps less than 9% of the total variance (Fig. 8, Online Supplemental Data File 11). Other holaspid morphs show similar results (Online Supplemental Data File 11). The major component of shape variation represented by RW1 is the arching of the whole pygidium and variations in the axis-direction distance between mid-posterior end of the pygidium and anterolateral tips of the pygidium (Fig. 8, Online Supplemental

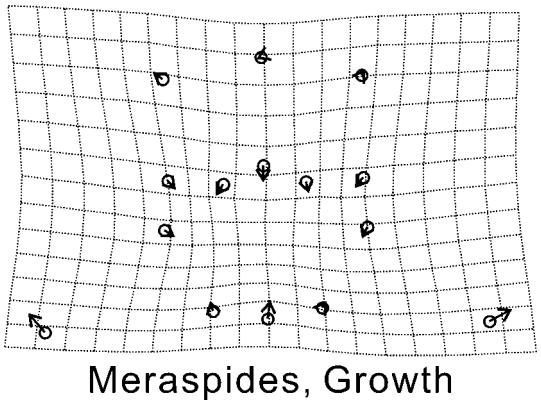

FIGURE 7—Thin-plate spline deformation grid of shape changes with growth for the 15 cranidial landmarks for specimens of meraspides from meraspid degree 4 through 17 (N=148). Partial warp scores are regressed in a multivariate regression against ln centroid size, and 7.6358% of total shape variance (based on summed squared residuals expressed in Procrustes units) is explained by the allometry (P<0.000625 from 1,600 bootstraps).

https://doi.org/10.1666/13-142 Published online by Cambridge University Press

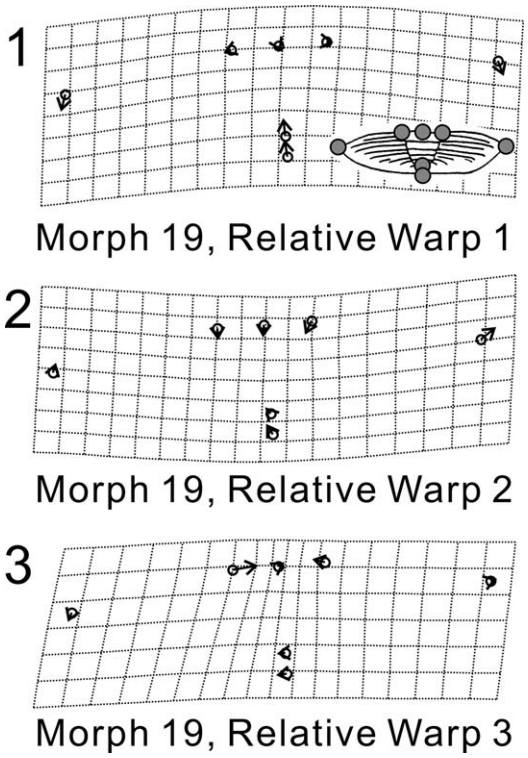

FIGURE 8—Thin-plate spline deformation grid of relative warps for the 7 pygidial landmarks for holaspid specimens of morph 19 with ln CCS value exceeding 2.2 (N=54): *1*, shape variation related to RW1 (54.03% of total variance explained); *2*, shape variation related to RW2 (14.78% of total variance); *3*, shape variation related to RW3 (13.19% of total variance).

Data File 11). RW2 represents variations in the relative length of the pygidium, and RW3 shows variations in the width of the pygidial axis.

There were some significant changes in the partial Procrustes distance with ln CCS for certain morphs (Fig. 9). For the morphs 19 and 21 specimens with ln CCS over 2.2 there was a significant slope value of 0.0241 (P=0.0395, r=0.0582) and 0.0262 (P=0.0044, r=0.2161) respectively. Slope values of morphs 18, 20, and 22 were not significant at the 95% confidence level (Online Supplemental Data File 11). Multivariate regression of partial warp scores against ln CCS for morphs 19 and 21 indicates that each growth vector explains 9.40% and 15.32% of the total variance respectively (Fig. 10), and the regressions were significant at P=0.001875 (1,600 bootstraps) and P=0.003750 (1,600 bootstraps) (Online Supplemental Data File 11). In addition, the vectors of regression coefficients for the morph 19 and for the morph 21 were significantly different from isometry at the 95% confidence level (morph 19: angle to isometry 99.1°, within-sample angle 46.7°; morph 21: angle to isometry 81.9°, within-sample angle 49.6°) (Online Supplemental Data File 11).

The major shape changes occurring with growth could not be simply linked to a single relative warp. However, the combined effect of relative warps could explain the arching (RW1 and RW2), shortening of axis (RW1 and RW2), and narrowing of axis (RW3) seen during holaspid pygidial growth.

Exoskeletal Growth 1: cephalic-trunk growth ratio.—As a basis for examining how the proportions of different components of the exoskeleton varied during growth the relative lengths of the major structural components of the exoskeleton were compared (Fig. 11). Using the antilogarithm of the regression coefficient (see Fusco et al., 2004) between the mean logarithm of the cranidial and exoskeletal lengths within meraspid degree 9

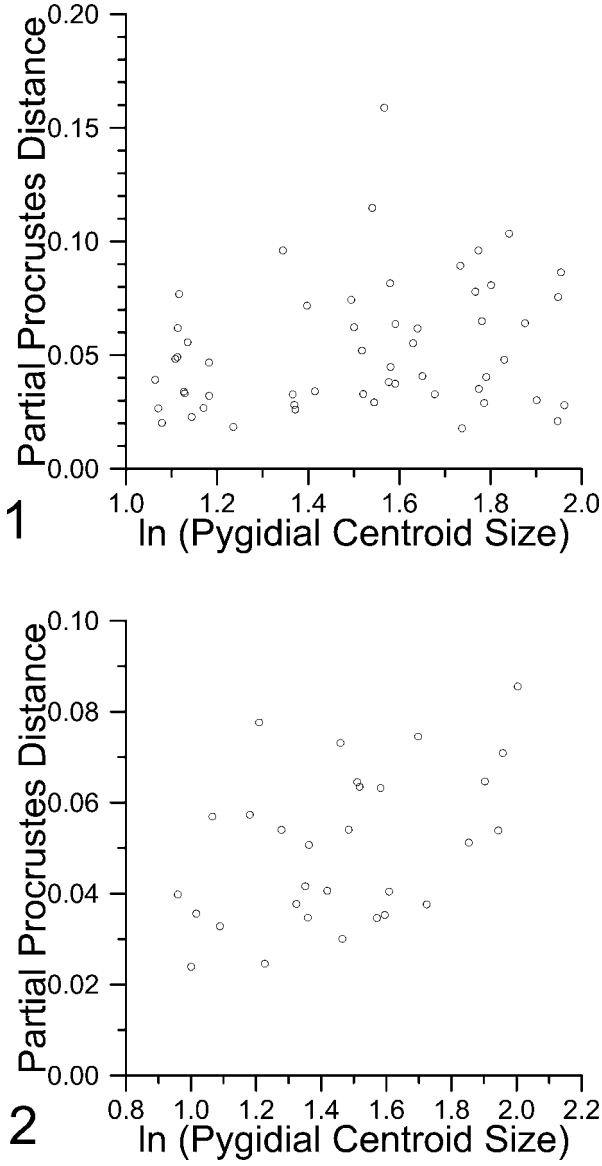

FIGURE 9—Partial Procrustes distance from the reference (mean shape of the smallest three specimens) of 7 pygidial landmarks for holaspid specimens of morph 19 (N=54) and morph 21 (N=30) with ln CCS value exceeding 2.2. Regression of partial Procrustes distance against logarithm of pygidial centroid size is significant. *1*, Morph 19 (slope=0.0241, P=0.0395, r=0.2412); *2*, Morph 21 (slope=0.0262, P=0.0044, r=0.4649).

through 17 as the basis for estimating growth rate, the cranidial length growth rate per meraspid stage 1.083 (1.080–1.089) is significantly lower than the exoskeletal growth rate 1.102 (1.095–1.110) (Fusco et al., 2004). Assuming a linear relationship between these variables (Fig. 11), the predicted cranidial-exoskeletal length ratio is 0.48 at meraspid degree 4, 0.44 at meraspid degree 9, and 0.39 at meraspid degree 17. This occurred in the context of cephalic growth taking place within a fixed set of segments, while trunk growth proceeded both by increase of segment size and the addition of new segmental units. The pattern of decrease in the cranidial:exoskeletal length ratio slowly declines with growth from –0.008 compared to previous instar at degree 4, to –0.006 at degree 17, and this decreased rate might have declined even more in the holaspid phase. Trunk length increase through segment addition had ceased at that point. Estimation of ratio changes in the holaspid phase (RMA regression used because both variables are independent of ln

https://doi.org/10.1666/13-142 Published online by Cambridge University Press

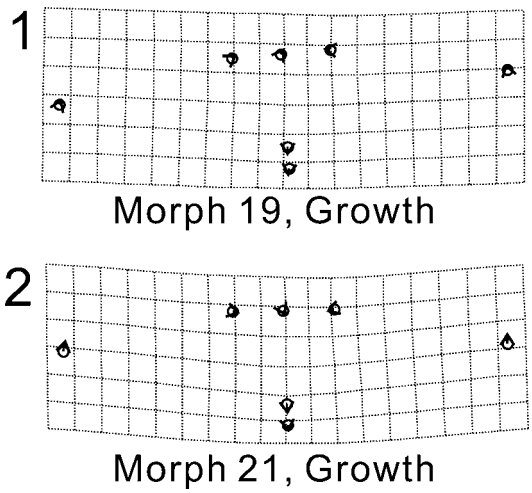

FIGURE *10*—Thin-plate spline deformation grid of shape changes with growth of 7 pygidial landmarks for holaspid specimens of morph 19 (N=54) and morph 21 (N=30) with ln CCS value exceeding 2.2. Partial warp scores are regressed in a multivariate regression against ln pygidial centroid size. *1*, Morph 19, 9.40% of total shape variance (based on summed squared residuals expressed in Procrustes units) is explained by the allometry (p=0.001875 from 1,600 bootstraps); *2*, Morph 21, 15.32% of total shape variance is explained by the allometry (P=0.003750 from 1,600 bootstraps).

cranidial length against ln exoskeletal length for morph 19 with ln CCS larger than 2.2) predicts values of 0.364 at exoskeletal length of 12 mm (which is about the exoskeletal length of the smallest morph 19 holaspides), and 0.358 at 20 mm (largest morph 19 holaspides).

In summary, the cephalic-trunk length ratio constantly decreases with growth from the meraspid phase to the holaspid phase, and the rate of decrease for the ratio values also seems to decrease as the species grows. This may imply that the amount of shape change per instar steadily decreased with growth, as these results do not reveal two separate rates of shape change for the meraspid and the holaspid phases.

Exoskeletal Growth 2: landmark-based analysis of exoskeletal shape.—The complex, ontogenetically dynamic nature of the trunk region complicates simple interpretation of its growth dynamics. Given the fact that among both different meraspid degrees and the various holaspid morphs the pygidium is homologous only as an articulation-defined unit (e.g., Hughes and Chapman, 1995), but not one that is homologous in terms of its constituent segments, we present analysis of exoskeletal growth to holaspides with 19 thoracic segments (morph 19) only, as it is the more numerous among morphs (but patterns seen within this morph are representative of those seen in the other well-represented morphs [Online Supplemental Data File 12]). The most noticeable modification is the modest ontogenetic expansion of the pygidium area compared to the cranidial region, most clearly indicated by the linear outward and forward trend in the positions of landmarks that represent the anterior lateral margins of the pygidium (Fig. 12).

Characteristics of holaspid shape variation can be further analyzed by the PCA of partial warp scores calculated from the mean shape of the sample. About 67.71% of the variance is explained by the first four relative warps, which account for between 23% to 12% of overall shape variance (Online Supplemental Data File 12). Shape changes seen in RW1 capture shape variations in the transverse extent of *A. koninckii*, previously seen in RW1 of the meraspid and holaspid phases of the cranidial dataset. RW2 seems to represent major shape variations related to growth, and it can be best summarized as a

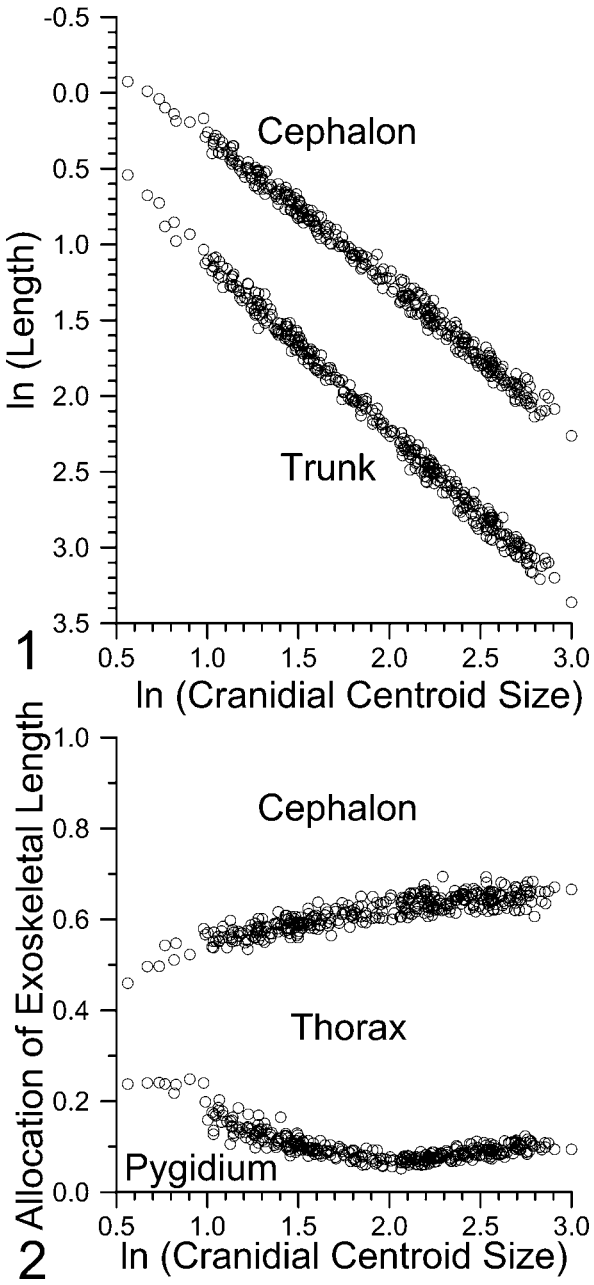

FIGURE *11*—Ontogenetic changes in length ratios of cephalon, thorax, and pygidium with growth for all meraspid and holaspid specimens (N=352): *1*, bivariate plot of ln cephalic length and ln trunk length against ln cranidial centroid size; *2*, changing proportion of the total length allocated to the cephalon, thorax, and pygidium.

difference in growth rates between the cranidial and pygidial regions (Fig. 13). RW3 shows similar variations seen in RW2 of cranidial meraspid and the cranidial holaspid phases, and also matches the growth vector of the cranidium. RW4 represents minor asymmetrical changes such as might result from compressional shearing. Other holaspid morphs also show similar shape variations (Online Supplemental Data File 12).

Shape change due to ontogeny can be evaluated by regressing partial Procrustes distances from a reference point (here the mean shape of the three smallest specimens) against ln CS (Fig. 14). Taking ln CS as an independent variable, the two show a significant positive relationship (r=0.4614, P<0.000625). The total shape variance is 0.0848, the residual, non-allometric shape

https://doi.org/10.1666/13-142 Published online by Cambridge University Press

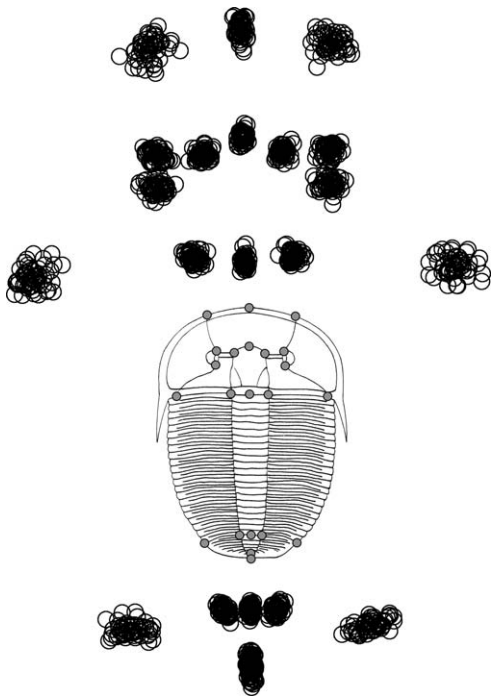

FIGURE 12—Procrustes superimposition of 22 exoskeletal landmarks for holaspid specimens of morph 19 with ln CCS value exceeding 2.2 (N=54).

variance is 0.0723, and 14.79% of the total variance is explained by the growth allometry ($P<0.000625$ from 1,600 bootstraps). The main allometric shape change is the expansion of the pygidial region compared to the cranidial area (Fig. 15), and this trend closely matches shape changes captured by RW2 in PCA of partial warp scores calculated from mean shape given immediately above. This, then, confirms that expansion of the relative size of the pygidium characterizes holaspid growth in this case. Other holaspid morphs display similar patterns of allometry (Online Supplemental Data File 12).

The significance of the allometric growth vector was tested by comparing its angle to an isometric vector with 1,600 bootstraps replicates. The result is that the within-sample angle (35.2°) is significantly different at the 95% confidence level to the angle-to-isometry (74.5°) Growth vectors of other morphs also showed significant differences from isometric growth (Online Supplemental Data File 12).

DISCUSSION

Exoskeletal shape change in *A. koninckii* is consistent with the pattern that is considered characteristic for trilobites: gradual, progressive change with the degree of allometry declining during ontogeny (Hughes et al., 2006). Although the transition from meraspid to holaspid growth in *A. koninckii* may coincide with a transition from weak allometric growth to isometry, there is little indication that this transition marked a profound change in cranidial growth dynamics. It did mark a transition in the growth of the trunk region, and particularly in the growth mode of the pygidium. Where allometry occurs, it is one of the major styles of variation present in the sample. Other common patterns of variation relate to the transverse aspect of specimens, and may reflect phenotypic variation or possibly compactional influence. Hints that a change may have occurred in the allometry of the eye do not receive statistical support, perhaps because subtle allometry is masked by minor taphonomic distortion. Although one of the holaspid segment number morphs does show significant allometry whereas others do not, we are hesitant to afford this observation much significance because the degree of size-related shape change is small, and because it is similar to that which occurs in the meraspid stage: there is no indication of the initiation of a significantly different growth mode.

Our results confirm the tight coordination of growth in *A. koninckii* and provide the oldest example of targeted growth in size and in shape yet known. They suggest that this species was able to adjust the growth of its size and shape rather precisely, presumably in order to conform to an optimal condition for each instar. A question that arises from this observation is how does this pattern of growth compare with other aspects of the development of *A. koninckii*?

Curiously, *A. koninckii* is well known for its remarkable variation in the number of thoracic segments found among holaspid specimens, with variants ranging from 18–22 thoracic segments (Hughes and Chapman, 1995). No other trilobite is known to show such a wide range of variation in mature segment numbers from a single locality, even among Cambrian trilobites where marked variation in thoracic segment numbers is quite common (Hughes et al., 1999). Previous studies of *A. koninckii* have considered the variation in mature segment number (Hughes and Chapman, 1995; Hughes et al., 1999; Fusco et al., 2004) and shown it not to be the result of lax developmental regulation, but rather that mature segment numbers were determined early in ontogeny, long before the transition into the holaspid phase. Hence, it appears that development in *A. koninckii* was able to forge morphologies of the appropriate size and shape, but also allowed for some versatility in the range of form produced at the end of anamorphosis. It remains unclear whether the five mature thoracic segment morphs each represent sibling species or rather were polymorphs of a single species. The fact that the cranidial trajectory of 19 is different from those of 20 and 21 might provide a basis for species distinction, but as the difference is subtle and characterizes one morph only we do not advocate this position. More importantly, in our view, all five morphs are extremely similar in form differing only in the total number of a structure expressed repeatedly and iteratively in all individuals.

Accordingly, *A. koninckii* apparently regulated its own development in a precise way. What, then, might explain the unusual variation in segment numbers evident in the sample? When considered in the context of independent evidence of the environmental conditions in which it thrived (Hughes et al., 2014), this growth pattern of *A. koninckii* may reflect its niche as an opportunistic species that flourished in conditions of reduced oxygen availability, and this issue will be considered in another work.

SYSTEMATIC PALEONTOLOGY

Order AULACOPLEURIDA Adrain, 2011

Remarks.—Adrain (2011) proposed the new order Aulacopleurida for trilobites with adult-like larvae that bear paired primary tubercles (a pattern recognized by Chatterton in 1980) on the dorsal exoskeleton during the protaspid and early meraspid phases, and assigned family Aulacopleuridae Angelin, 1854 and fourteen other families to the order.

Family AULACOPLEURIDAE Angelin, 1854

Remarks.—Aulacopleuridae differs from other families of Aualcopleurida in its subquadrate hypostome with paired posterior spines, the bilobate eye socle, the presence of a thoracic axial spine in some groups, and its relatively wide and short pygidium (Adrain and Chatterton, 1993). Subfamilies Aulacopleurinae and Otarioninae comprise the family.

https://doi.org/10.1666/13-142 Published online by Cambridge University Press

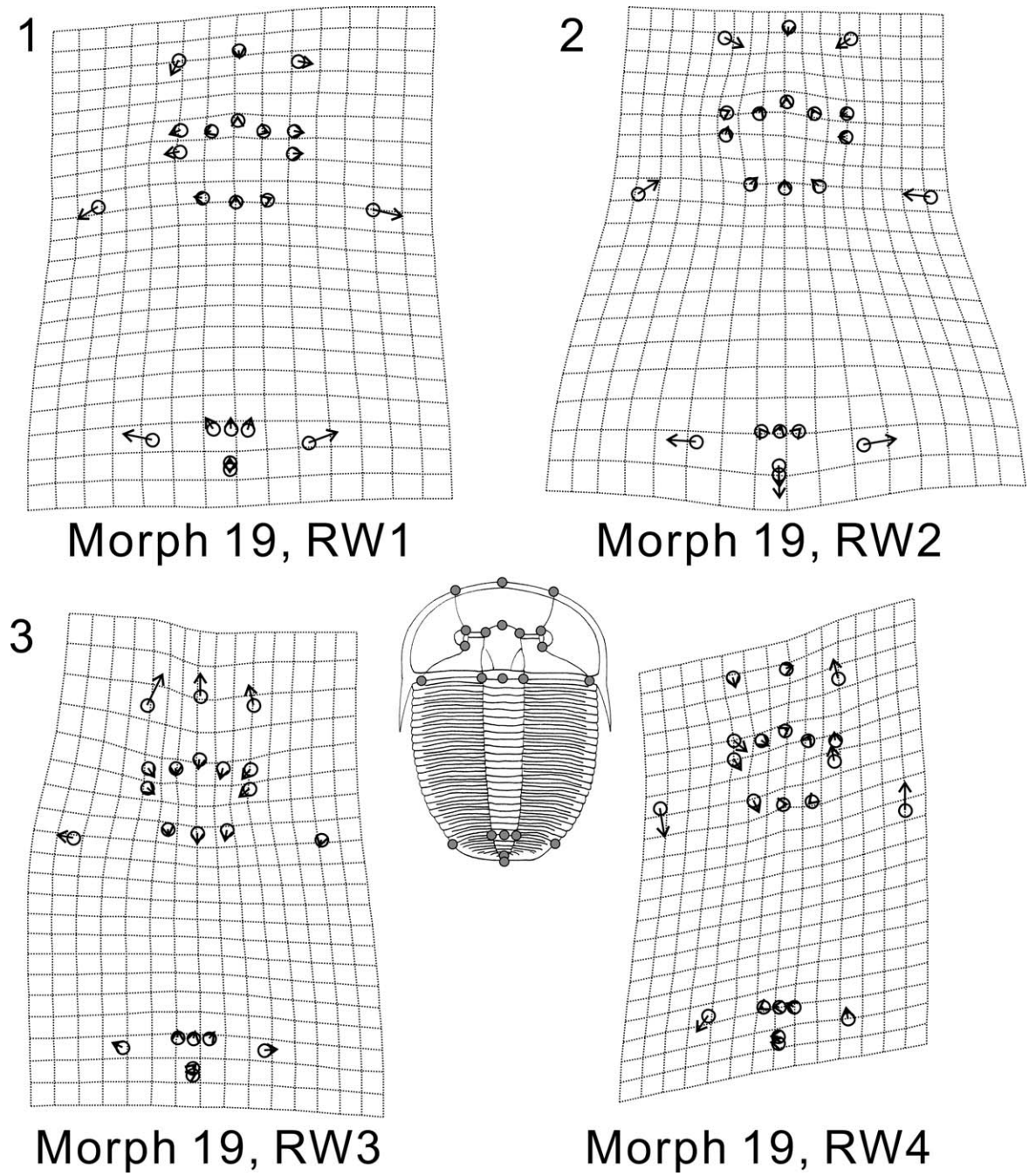

FIGURE *13*—Thin-plate spline deformation grid of relative warps of 22 exoskeletal landmarks for holaspid specimens of morph 19 with ln CCS value exceeding 2.2 (*N*=54): *1*, shape variation related to RW1 (22.94% of total variance); *2*, shape variation related to RW2 (16.71% of total variance, direction inversed); *3*, shape variation related to RW3 (15.90% of total variance); *4*, shape variation related to RW4 (12.16% of total variance).

Subfamily AULACOPLEURINAE Angelin, 1854

Remarks.—Compared to the subfamily Otarioninae, the primary paired tubercles of Aulacopleurinae are subdued or absent in early ontogenetic stages, the hypostome is elongated with a narrow middle body, the pleural area is wider, and genal caeca are stronger (Adrain and Chatterton, 1993). A pioneering study of phylogenetic relationships within the Aulacopleurinae (Yuan et al., 2001) suggested that the subfamily comprises two clades, one of which contains species referable to genera *Paraaulacopleura* Chaubet, 1937 and *Songkania* Lu, 1975 and which share relatively long and narrow pygidia, and another which comprises species attributable to *Aulacopleura* Hawle and Corda, 1847 characterized by anteriorly positioned eyes and small pygidia. Yuan et al. (2001) argued that the diagnostic characters of *Aulacopleura* were the result of peramorphic evolution, although evidence for allometric change in these characters within *A. koninckii* is unclear because the position of the eyes remains constant with growth, and we lack data on ontogeny and ancestor-descendant relationship of the other species.

Genus AULACOPLEURA Hawle and Corda, 1847

1846a *Arethusa* BARRANDE, p. 48.
1847 *Aulacopleura* HAWLE and CORDA, p. 84.
1852 *Arethusina* BARRANDE, p. 493.

https://doi.org/10.1666/13-142 Published online by Cambridge University Press

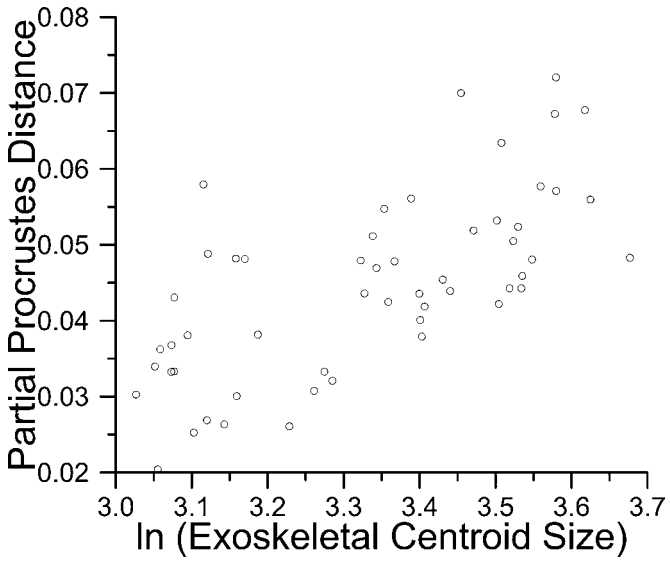

FIGURE 14—Partial Procrustes distance from the reference (mean shape of the smallest three specimens) of 22 exoskeletal landmarks for holaspid specimens of morph 19 with ln CCS value exceeding 2.2 (N=54). Regression of partial Procrustes distance against logarithm of cranidial centroid size is significant (slope=0.0425, $P<0.0001$, r=0.6792).

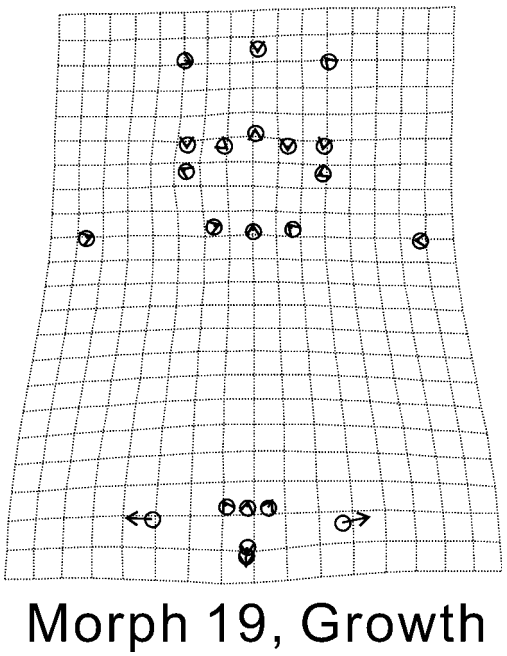

FIGURE 15—Thin-plate spline deformation grid of shape changes with growth of 22 exoskeletal landmarks for holaspid specimens of morph 19 with ln CCS value exceeding 2.2 (N=54). Partial warp scores are regressed in a multivariate regression against ln centroid size, and 14.7893% of total shape variance (based on summed squared residuals expressed in Procrustes units) is explained by the allometry ($P<0.000625$ from 1,600 bootstraps).

1947 *Aulacopleura* (*Aulacopleura*); PŘIBYL, p. 539.
1978 *Otarion* (*Aulacopleura*); THOMAS and OWENS, p. 68.

Diagnosis.—Preglabellar area long with glabella occupying less than 60% of cephalic length; eyes small, exsagittal length less than 40% of glabellar length, anteriorly located with its anterior opposite no less than 75% of the glabellar length from its posterior margin forward. Pygidium wide and short, more than thrice as wide as long.

Type species.—*Arethusa koninckii* Barrande, 1846a, *Testograptus testis* Zone of upper Motol Formation, Wenlock (lower Homerian), *Arethusina* Gorge in Velká Ohrada, Prague-Řeporyje District, Czech Republic (by monotypy).

Other species.—*Aulacopleura andersoni* Adrain and Chatterton, 1995, Llandovery (Telychian), the central Mackenzie Mountains, Canada; *A. krizi* Šnajdr, 1975, Llandovery (uppermost Aeronian), Hýskov near Beroun, Czech Republic; *A. pogsoni* Edgecombe and Sherwin, 2001, Llandovery (lower Telychian), Cotton Hill, New South Wales, Australia; *A. soror* Přibyl, Vaněk, and Hörbinger, 1985, Wenlock (lower Homerian), Herinky Hill near Lištice, and Vyskočilka near Malá Chuchle, Czech Republic; *A. wulongensis* Wang, 1989, Llandovery (Aeronian), near Tongzi, Sichuan Province and Hubei Province, China (Yuan et al., 2001).

Otarion burmeisteri var. *hercynica* Kegel, 1928 is based on a single cranidium specimen found from a limestone lens of the Wieder Shales in the Wieda Valley near Zorge, Harz Mountains, Germany. Přibyl and Vaněk (1981) later considered this Ludlovian taxon to species rank within *Aulacopleura* but without giving a justification. *Aulacopleura* (*A.*) *bohemica* Přibyl, 1947 is recorded from the Middle Devonian Slivenec Limestone in Koněprusy near Beroun, Czech Republic. Both taxa are only known from drawings (Kegel, 1928, pl. 32, fig. 6; Přibyl, 1947, pl. 10, figs. 1–10), and we refrain from making a taxonomic judgement on them.

Arethusa nitida Barrande, 1846b was established based on a single pygidium from the Kozel Limestone near Beroun, Czech Republic by Barrande (1846b). The specimen probably came from the beds 24 and 25 of the Kozel Limestone in the U Drdů section (No. 760), Berounka Valley near Lištice, and these beds correlate to the *Pristiograptus dubius parvus* Zone of the uppermost Homerian, Wenlock (Kříž et al., 1993). Additional materials including cranidia from the same beds were later identified by Přibyl et al. (1985) as *Nitidocare nitidum* (Barrande, 1846b). The species has a subquadrate glabella with deeply incised S1 and S2, and is referable to the family Rorringtoniidae Owens and Hammann, 1990. Specimens described by Horný et al. (1958) as *Aulacopleura* (*A.*) *nitida* were later assigned to *Aulacopleura soror* Přibyl et al., 1985.

Aulacopleura socialis Poulsen, 1934 occurs in the Cape Schuchert Formation in Washington Land, north Greenland, and in the *S. turriculatus* Zone of the Road River Formation, Llandovery (lower Telychian), from the gorge of Prongs Creek, northern Yukon Territory, Canada (Ludvigsen and Tripp, 1990). The species has distinct anteriorly diverging facial sutures, and should be assigned as a species of genus *Songkania*.

Aualcopleura? *ranfordi* Adrain and Chatterton, 1995 is from the *Distomodus kentuckyensis–Icriodela discrete–Oulodus*? *nathani* Zone of the Whittaker Formation, Llandovery (earliest Rhuddanian), the central Mackenzie Mountains, Canada. The species is older than any other known species of *Aulacopleura*, and we concur with the authors that it may represent a separate, closely related clade to the genus *Aulacopleura* based on differences its shorter frontal area, narrower pleural regions, and longer pygidium.

Remarks.—More than 20 species and subspecies have been assigned to the genus or subgenus *Aulacopleura* (Prantl and Přibyl, 1950; Thomas, 1978; Přibyl and Vaněk, 1981; Wang, 1989; Adrain and Chatterton, 1995; Edgecombe and Sherwin, 2001; Yuan et al., 2001). The subgenus *Aulacopleura* (*Paraaulacopleura*) was established by Chaubet (1937) with the Wenlockian *Aulacopleura* (*Paraaulcopleura*) *roquemaillerensis* from Montage Noire as the type species. *Paraaulacopleura* is now treated as a genus-level taxon (Jell and Adrain, 2003), and the species in that genus differ from *A. koninckii* by having a shorter preglabellar field, more posteriorly located eyes

https://doi.org/10.1666/13-142 Published online by Cambridge University Press

associated with eye ridges that sweep posteriorly abaxially, and a longer pygidium. *Aulacopleura koninckii* and *Paraaulacopleura roquemaillerensis* are broadly representive of the two morphologically distinct groups of taxa that have been referred to as species or subspecies of Aulacopleurinae (Schindewolf, 1924; Chaubet, 1937; Přibyl, 1947; Adrain and Chatterton, 1995). Only taxa complying with the diagnosis given above are here considered species of *Aulacopleura*, and consequently this confines occurrence of the genus to the Llandovery and Wenlock only, occurring most commonly in relatively basinward sedimentary rocks distributed about the margins of the paleo-Tethyan ocean. The remaining species, predominently Devonian in age, belong within in *Paraaulacopleura* or *Songkania*. Although in overall form Ordovician aulacopleurines with shorter frontal areas and posteriorly positioned eyes resemble *Paraaulacopleura* species more closely than those in *Aulacopleura*, Yuan et al., (2001) argued that early forms differ in having shorter pygidia, a plesiomorphic character that members of *Aulacopleura* retain.

AULACOPLEURA KONINCKII (Barrande, 1846a)
Figures 16–20

1846a *Arethusa Koninckii* BARRANDE, p. 48.
1847 *Aulacopleura koninckii* (Barrande); HAWLE and CORDA, p. 85, pl. 5, fig. 48.
1852 *Arethusina Koninckii* (BARRANDE), p. 495, pl. 18, figs. 1–21.
1887 *Arethusina Haueri* FRECH, p. 736, pl. 29, fig. 11.
1895 *Arethusina Koninckii* var. *peralta* KATZER, p. 8, pl.1, figs. 3, 3a, 3b, 3c.
non1937 *Aulacopleura Koninckii* var. *occitanica* CHAUBET, p. 192, pl. 7, figs. 4, 6.
1947 *Aulacopleura* (*Aulacopleura*) *koninckii koninckii* (Barrande); PŘIBYL, p. 539, pl. 80, figs. 11, 12.
1950 *Aulacopleura* (*Aulacopleura*) *koninckii koninckii*; PRANTL and PŘIBYL, p. 404, pl. 1, figs. 20–24, pl. 3, fig. 7 (synonymy to date).
1950 *Aulacopleura* (*Aulacopleura*) *koninckii haueri* (Frech); PRANTL and PŘIBYL, p. 493–494, pl. 2, figs. 1–3, pl. 5, fig. 7 (synonymy to date).
1957 *Aulacopleura* (*Aulacopleura*) *koninckii* (Barrande); TOMCZYKOWA, p. 132, pl. 3, figs. 1, 2 (synonymy to date).
1970 *Aulacopleura* (*Aulacopleura*) *koninckii koninckii*; HORNÝ and BASTL, p. 183, pl. 12, fig. 2.
1978 *Otarion* (*Aulacopleura) koninckii* (Barrande); THOMAS and OWENS, p. 68, fig. 10.
1990 *Aulacopleura koninckii* (Barrande); ŠNAJDR, p. 22, p. 40, p. 176.
1993 *Aulacopleura koninckii*; KŘÍŽ ET AL., p. 814, p. 820.
1995 *Aulacopleura koninckii*; HUGHES and CHAPMAN, figs. 1.A–1.H, 1.K–1.L, 5, 6.
1999 *Aulacopleura koninckii*; HUGHES ET AL., fig. 3a–3c.
2001 *Aulacopleura koninckii haueri* (Frech); SANTEL, p. 119, pl. 5, figs. 1–6.
2003a *Aulacopleura koninckii*; HUGHES, fig. 3A.
2003b *Aulacopleura koninckii*; HUGHES, fig. 2A.
2004 *Aulacopleura koninckii*; FUSCO ET AL., fig. 2.
2005 *Aulacopleura koninckii*; HUGHES, fig. 3A.
2007 *Aulacopleura koninckii*; HUGHES, fig. 1.
2008 *Aulacopleura koninckii*; HUGHES ET AL., fig. 15.2.
2014 *Aulacopleura koninckii*; FUSCO ET AL., figs. 1, 2.
2014 *Aulacopleura koninckii*; HUGHES ET AL., figs. 6A, 7, 10, 12–14.

Diagnosis.—*Aulacopleura* with 18–22 thoracic segments in the holaspid phase; narrow subrectangular glabella that weakly tapers anteriorly; hypostome with constriction at the anterior portion of the middle body; small eyes with sagittal length shorter than half of glabellar length throughout ontogeny, anterior of eye opposite lateral margin of preglabellar furrow.

Holaspid description.—Exoskeleton ovate in outline; cranidial width across posterior border about 65% of sagittal length.

Cephalon semicircular in outline; sagittal length about 55% of cranidal width across posterior border; sagittal length about 35% of exoskeletal sagittal length. Cephalon convex; glabella and occipital lobe (LO) maintain curvature of genal field. Anterior genal field slopes gently ventrally compared to steeper lateral genal field. Posterior genal field slopes steeply adaxially. Caecal pits spaced evenly throughout genal field, roughly equal number of pits throughout growth; pits apparently slightly smaller on posterior fixigenae, about 40 pits per 1 mm^2 in specimen with cranidial length 5.6 mm. Anterior and lateral cephalic border narrow, tubular. Anterior cephalic border arched dorsally in anterior view. Medial notch in dorsal view variably expressed, ranging from absent to prominent. Posterior cephalic border shortens (exsag.) adaxially. Anterior and lateral cephalic border furrows very short (sag., exsag.), moderately to weakly incised, narrow (tr.). Posterior cephalic border furrow lengthens (exsag.) abaxially. Genal spine directed posteriorly, length about twice width (tr.) of lateral cephalic border at base, tapered evenly, continuing curvature of cephalic outline. Anterior branches of facial suture diverge at 20° to axis anteriorly, rapidly converge toward 90° to axis slightly before reaching border furrows. Posterior branches of facial suture diverge at 60° to axis posteriorly; terminate at posterior cephalic margin. Frontal area length about 45% of cranidial length.

Holochroal eyes small, kidney-shaped; length about 15% of cranidial length. Anterior end of eye located at about 85% of glabellar length from its posterior margin forward. Posterior end of eye located at about 50% of glabellar length from its posterior margin forward. Distance of eye to axis about 40% of cranidial width across posterior border. Eye surface and palpebral lobe hemispherical, upstanding. Base of hemisphere elevated vertically above genal field on eye socle about half the height of hemisphere. Eye socle and eye socle furrow continuous in curvature. Visual field spans slightly below horizontal plane to 90° above it. Overlap of visual fields from paired eyes about 35° at front and back. Hexagonal close packing of lenses with at least 20 lenses at basal horizontal row and at least 20 horizontal rows of lenses. Eye ridge orthogonal to sagittal axis; intersects anterior portion of eye and lateral margin of preglabellar furrow. Lateral axial furrows narrow (tr.), very deeply incised, gently bowed abaxially around L1; preglabellar furrow gently arching anteriorly.

LO anterior arched forward sagittally. Maximum LO length about 10% of cranidial length. Cephalic median organ quincuncial; occurs as four small outer tubercles and a larger central one on flat surface, located slightly anterior to sagittal mid-point of LO. SO deepest near axial furrow; shallowing sagittally. Glabella trapezoidal in outline. Sagittal anterior curvature of glabella continuous with that of preglabellar field and of LO. Glabella widest at posterior of first glabellar lobe (L1). Glabellar length and width about 45% and 25% of cranidial length and width, respectively. Width of anterior glabella across eye ridges about 75% of maximum glabellar width. Glabella tapering anteriorly at about 5° to sagittal axis. L1 teardrop shaped, slightly expanded laterally. S1 deep near lateral axial furrow, shallowing adaxially, fully isolating L1, in contact with medial SO. L2 very weakly incised as small notch opposite middle (exsag.) of eye.

Hypostome subrectangular. Maximum width near posterolateral margin, at about 65% of sagittal length. Anterior margin

https://doi.org/10.1666/13-142 Published online by Cambridge University Press

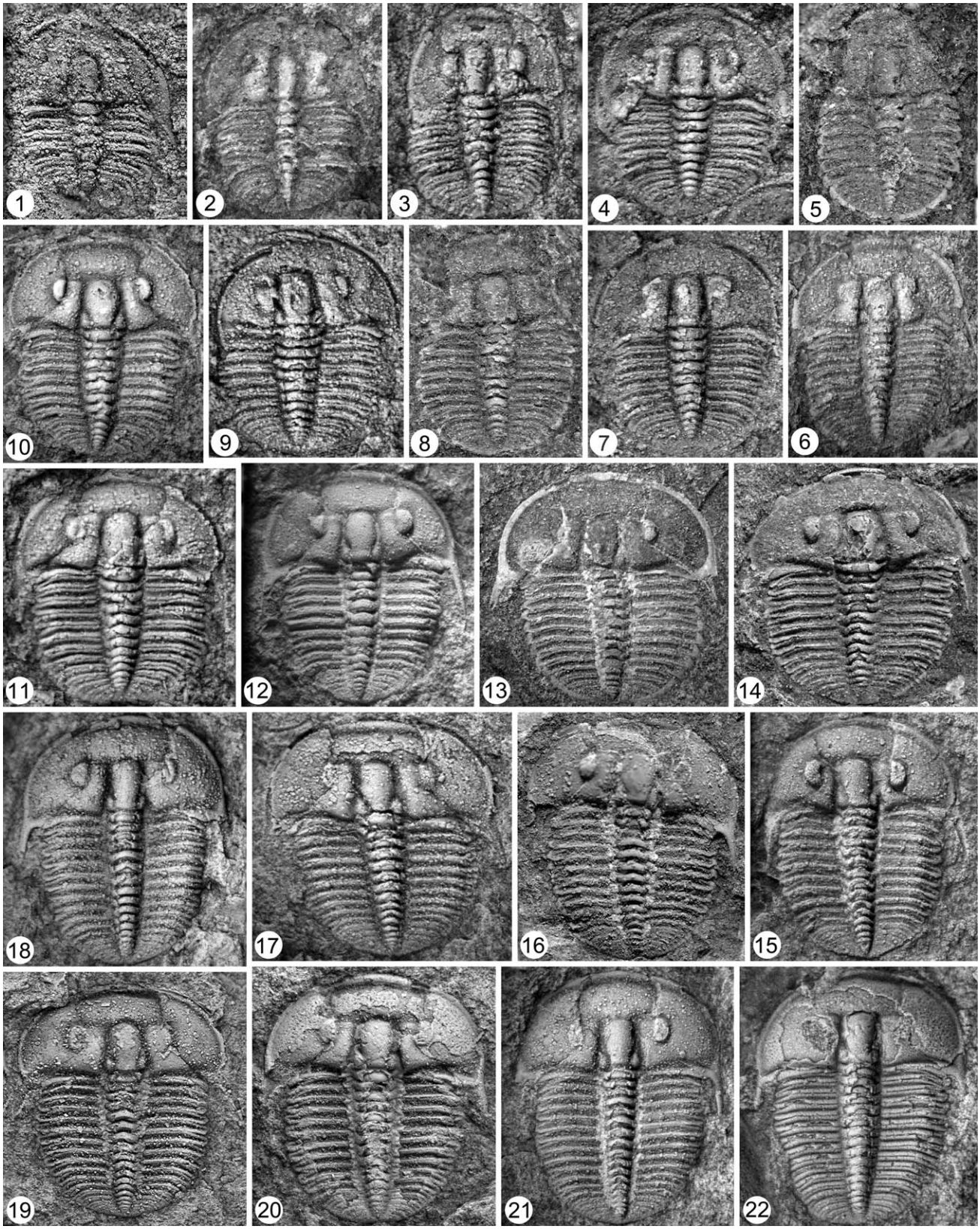

FIGURE *16—Aulacopleura koninckii* (Barrande, 1846a) from Na Černidlech, Czech Republic; specimens coated with magnesium oxide prior to photography: *1*, meraspid degree 4, MCZ177964 ×16.4; *2*, meraspid degree 4, NMPL39407 ×15.2; *3*, meraspid degree 5, NMPL40040A ×15.6; *4*, meraspid degree 5, NMPL39950 ×15.2; *5*, meraspid degree 6, BMNH42364.3 ×13.6; *6*, meraspid degree 6, NMPL39916 ×12.0; *7*, meraspid degree 6, NMPL2234 ×14.0; *8*, meraspid degree 7, BMNH42364.1 ×12.0; *9*, meraspid degree 7, NMPL2243 ×15.6; *10*, meraspid degree 8, NMPL39957 ×12.0; *11*, meraspid degree 8, NMPL40082 ×14.4; *12*, meraspid degree 9, NMPL40035 ×11.2; *13*, meraspid degree 9, NMPL39924 ×10.8; *14*, meraspid degree 9, MCZ116103 ×11.2; *15*, meraspid degree 10, NMPL40028 ×10.0; *16*, meraspid degree 10, BMNH42365.5 ×10.4; *17*, meraspid degree 10, NMPL39949 ×10.0; *18*, meraspid degree 11, NMPL40079 ×9.6; *19*, meraspid degree 11, NMNH475176 ×8.8; *20*, meraspid degree 11, MCZ116205 ×9.2; *21*, meraspid degree 12, NMPL39961 ×8.8; *22*, meraspid degree 12, NMPL40023 ×8.8.

https://doi.org/10.1666/13-142 Published online by Cambridge University Press

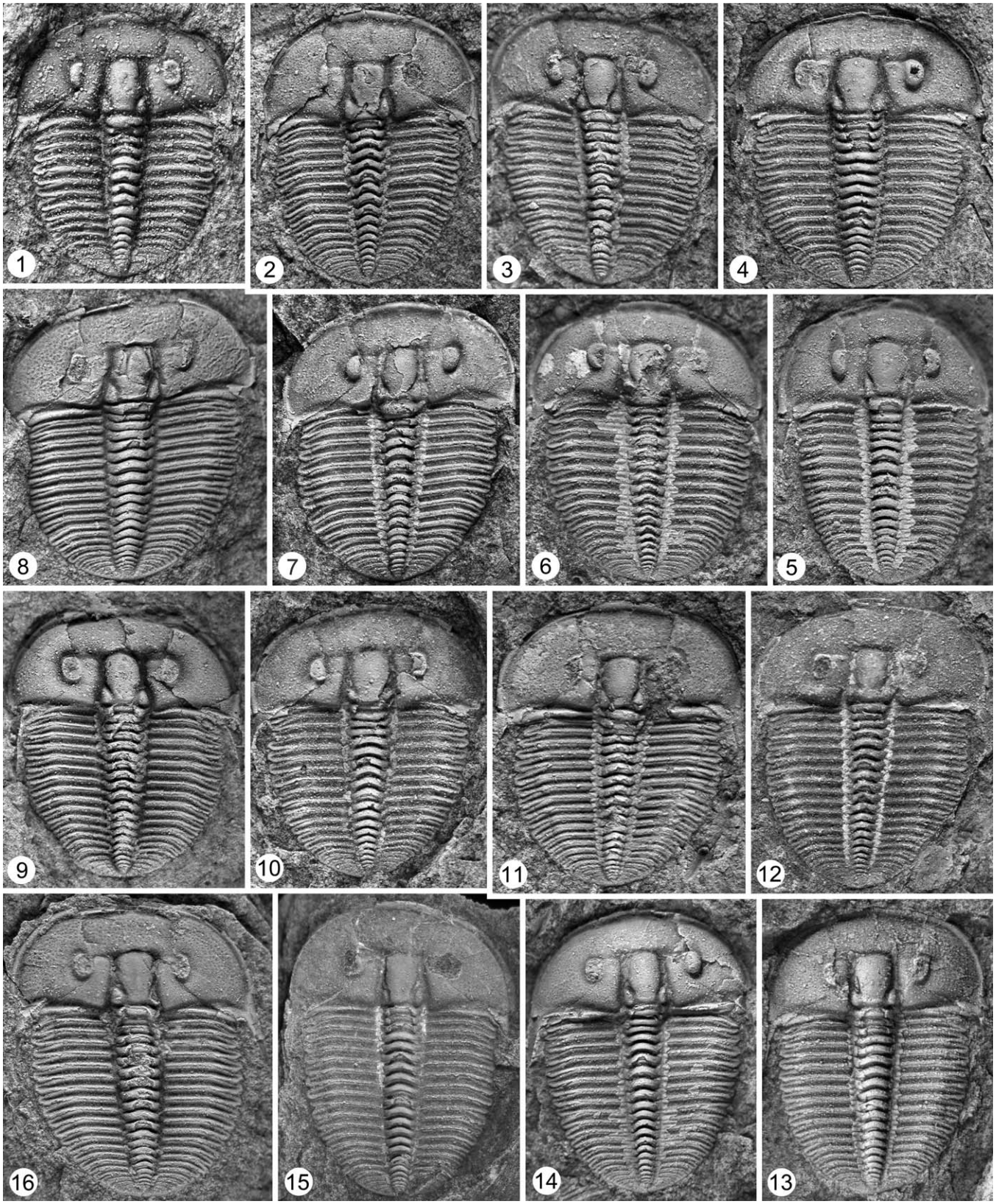

FIGURE 17—*Aulacopleura koninckii* (Barrande, 1846a) from Na Černidlech, Czech Republic; specimens coated with magnesium oxide prior to photography: *1*, meraspid degree 12, BMNH42365 ×10.8; *2*, meraspid degree 13, MCZ177963 ×7.6; *3*, meraspid degree 13, MCZ115992 ×8.4; *4*, meraspid degree 13, MCZ116201 ×8.8; *5*, meraspid degree 14, MCZ115990 ×7.6; *6*, meraspid degree 14, MCZ115987 ×7.2; *7*, meraspid degree 14, MCZ177744 ×8.0; *8*, meraspid degree 15, MCZ114948 ×7.6; *9*, meraspid degree 15, NMNH475182(475181) ×6.4; *10*, meraspid degree 15, MCZ116186 ×8.0; *11*, meraspid degree 16, MCZ114936 ×6.8; *12*, meraspid degree 16, MCZ116055 ×6.8; *13*, meraspid degree 16, NMPL40073 ×6.8; *14*, meraspid degree 17, MCZ115406 ×6.0; *15*, meraspid degree 17, MCZ116087 ×6.0; *16*, meraspid degree 17, MCZ177982 ×6.4.

https://doi.org/10.1666/13-142 Published online by Cambridge University Press

gently arching anteriorly in the middle, extended into long (exsag.) anterior wings laterally. Lateral margin parallel to sagittal axis posterior to about 35% of sagittal length from anterior, slightly divergent posteriorly at about 60% of sagittal length from anterior. Posterior margin semicircular to trapezoidal. Posterolateral spines absent. Anterior border as long as posterior border at sagittal axis; abruptly lengthens abaxially near anterior wing, continuous with anterior lobe and anterior wing. Lateral border slopes steeply into lateral border furrow. Lateral border slightly narrower than long (sag.) posterior border. Posterior border uniform in length, flange-like. Lateral and anterior border furrows converge anteriorly at about 30° to sagittal axis at anterolateral corners behind anterior wing, deep, trough-like, uniformly wide; defining bottleneck shaped anterior lobe. Lateral border furrow deeply incised, narrow opposite anterior lobe, as wide as posterior border furrow at posterolateral region. Posterior border furrow deep, uniformly long. Middle body constricted at about 20% of sagittal length anterior of posterior margin to minimum width of about 65% of maximum middle body width, slightly inflated transversely anterior to narrowest position. Middle body length about 90% of hypostomal sagittal length. Middle body width about 70% of hypostomal maximum width near posterolateral margin. Surface sculpture weakly defined fingerprint-like pattern. Middle furrow slit-like on internal mold, converging posteriorly at about 45° to sagittal axis opposite inflection point of lateral border, isolated from sagittal axis.

Trunk with homonomous segments. Number of thoracic segments in holaspid/epimorphic forms ranges from 18–22. Thoracic length about 55–60% of exoskeletal length with segment-poor specimens closer to about 55% and with segment-rich ones closer to about 60%. Maximum length and width of trunk at seventh segment from trunk anterior. Ratio of axial to pleural width about 25% near middle. Outer portion of pleura beyond fulcrum about 40% of pleural width. Pleural furrow long (exsag.) and parallel to segment margin in inner portion, shortening (exsag.) abaxially in outer portion. Length of posterior band increases abaxially in outer portion of pleura. Pleural extremity of anterior segments developed into pointed tip, more rounded in posterior segments. Axial ring arched anteriorally at sagittal axis, flexing posteriorly abaxially, but curving anteriorly near axis to form weak W shape in dorsal view. Weak median tubercle visible in some segments. Articulating furrow short (sag. and exsag.).

Pygidium semielliptical with sagittal length about 25% of maximum width. Pygidial border narrow, of uniform thickness. Pygidial border furrow very shallow and narrow. Inner portion of pleural field dorsally flat, width between fulcra at thoracopygidium boundary about 65% of maximum pygidial width. Up to four pairs of pleural furrows, more prominent anteriorly, where deep and wide. Anterior band length about 50% of posterior band at inner portion of pleural field, about the same length at outer portion of pleural field. Up to four pairs of interpleural furrows, deep, narrow at inner portion of pleural field; widening abaxially at boundary of pleural field. Relation between axial and pleural portions of segments moderately clear. Pygidial axis conical in outline, sides gently converging posteriorly. Posterior portion broadly rounded. Length of pygidial axis about 80% of pygidial length. Width of pygidial axis about 20% of maximum pygidial width. Axis composed of four to up to six axial rings and a terminal axial piece. Inter-ring furrows short (sag. and exsag.), firmly incised, slightly arched anteriorly.

Ontogeny.—Other than the addition of trunk segments in the meraspid phase, and the complementary release of anterior pygidial segments into the thorax, no other ontogenetic changes in nominal or ordinal characters could be detected from meraspid degree 4 to the largest holaspid. Trunk segment development is synarthromeric. Such changes as do occur are related to the overall sizes of individual sclerites, the numbers of trunk segments, and their allocation to the pygidium or thorax.

As described above, during the meraspid phase the relative length of the cranidial frontal area expands, the front of the glabellar becomes less rounded, and the posterior broader widens and moves slightly anteriorly. Thus in larger forms, the glabella and eyes are relatively smaller than those of earlier meraspides.

With regard to the overall shape of the exoskeleton, the major ontogenetic change is the expansion of the area occupied by the thorax during meraspid ontogeny, and the relative decline in the size of the pygidium during this phase. This decline is related to the fact that although the pygidium increased in size during the meraspid phase, such increase was mitigated by loss of the anteriormost pygidial segment into the thorax at each meraspid molt. Thus, as a proportion of the total exoskeleton, the pygidium became both narrower and shorter during later meraspid growth. This growth relationship changed during the holaspid phase because the pygidium was no longer releasing or adding segments, and its constituent segments thus increased in size. For details of individual trunk segment growth rates see Fusco et al. (2014).

Types.—The original specimens referred to in Barrande's paper (1846a) are from a locality in "Wohrada" which is the current *Arethusina* Gorge, Velká Ohrada of the Prague-Řeporyje District, Czech Republic (Kříž et al., 1993). According to Horný and Bastl (1970, p. 183), this material consisted of five specimens that are stored at the National Museum of Prague. Prantl and Přibyl (1950, p. 491) designated the specimen figured in the later work of Barrande (1852, pl. 18, figs. 16, 17) as a lectotype without specifying a specimen number. The locality of the specimen in question is also recorded as "Wohrada" (Barrande, 1852, pl. 18 captions), but it is uncertain whether it was one of the five specimens referred to by Barrande (1846a). Currently, the specimen cannot be located within the Museum. Of the five original specimens, two (NMP L2289 and NMP L2236) are known by specimen numbers (Horný and Bastl, 1970, p. 183), and only L2236 could be located. Consequently, the later designation of specimen NMP L2022 (IT278) as neotype by Horný and Bastl (1970, p. 185) was erroneous. In addition, specimen L2022 (IT278) is from a different locality, that of Na Černidlech Hill, Loděnice, Beroun District (Horný and Bastl, 1970, p. 185). Therefore, specimen L2236, a complete, partially exfoliated exoskeleton (Fig. 20.7), is here designated as the lectotype.

Occurrence.—The Wenlockian, central European species occurs in outcrops of the *T. testis* Zone of the type locality and the Central segment of the Barrandian exposed between Svatý Jan and Prague; the species is best known from the Na Černidlech Hill locality in the *Aulacopleura* shales, upper 1.4 meter interval of the Motol Formation, *T. testis* Zone, Homerian, Wenlock, Silurian. In addition, Katzer's (1895) variety *Arethusina koninckii* var. *peralta* from the Kozel Limestone, Berounka Valley, Lištice, Beroun District extends the species's range into the Homerian *P. dubius parvus* Zone, which overlies the *T. testis* Zone in the upper Motol Formation (Kříž, 1992; Kříž et al., 1993).

Occurrences outside the Czech Republic are as follows: *Cryptograptus lundgreni* Zone (correlation from Kříž, 1999, p. 305), Orthocerankalk, Wenlock (lower Homerian), Rauchkofel and other regions of the Carnic Alps, southern Austria (Frech, 1887; Hertisch, 1929; Gärtner, 1930; Santel, 2001); *Cryptograptus perneri* and *C. lundgreni* zones, Wenlock (lower Sheinwoodian), Mójcza, near Kielce, Świętokrzyskie Province, Holy Cross Mountains, south-central Poland (Tomczykowa, 1957).

A distorted cranidial specimen from the Wenlockian (lowermost Sheinwoodian) *Cryptograptus centrifugus* Zone at the

https://doi.org/10.1666/13-142 Published online by Cambridge University Press

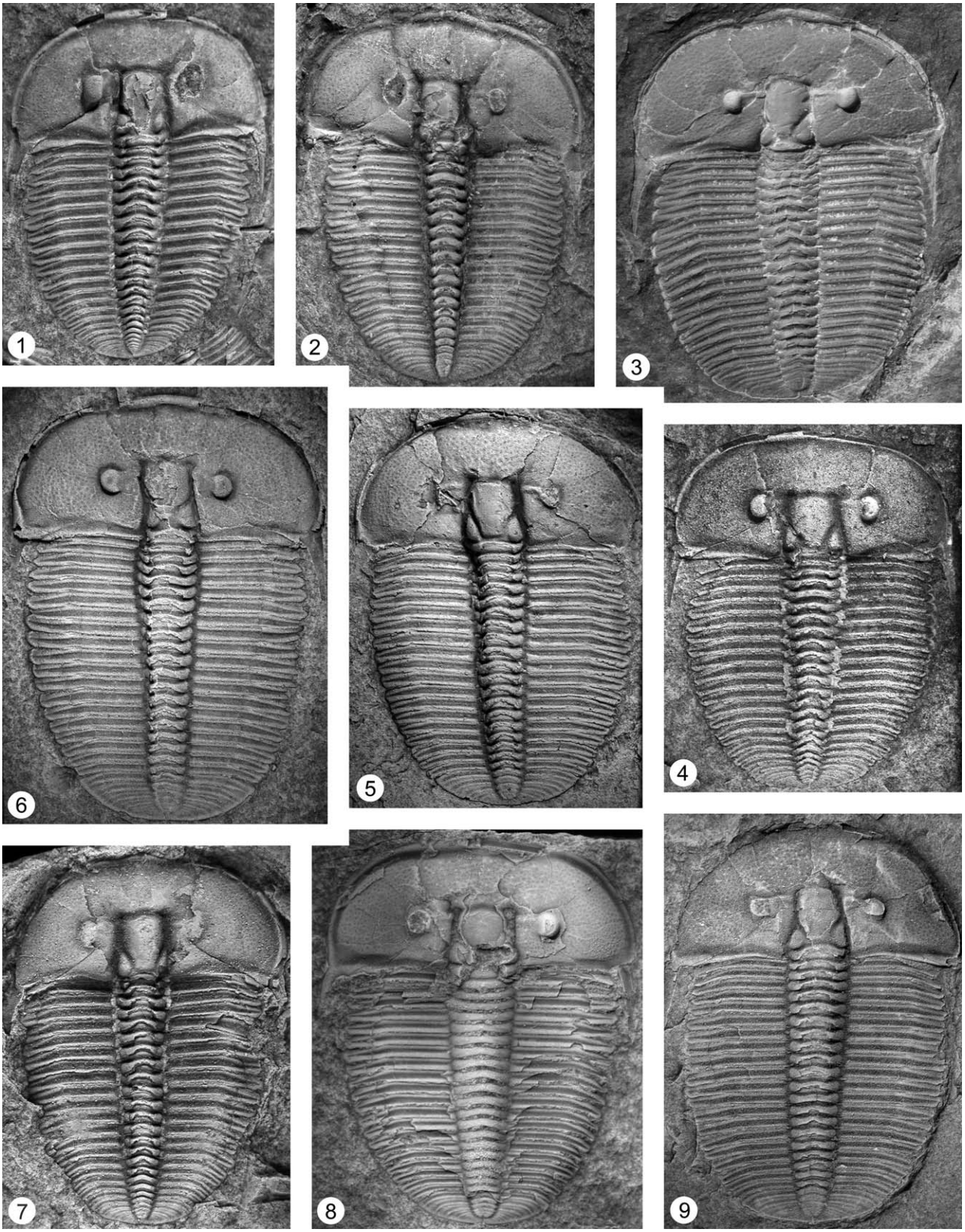

FIGURE *18*—*Aulacopleura koninckii* (Barrande, 1846a) from Na Černidlech, Czech Republic; specimens coated with magnesium oxide prior to photography: *1*, 18 thoracic segments, MCZ116174 ×6.5; *2*, 18 thoracic segments, BMNH59826.6 ×3.7; *3*, 18 thoracic segments, NMPL2229 3.×2.7; *4*, 19 thoracic segments, MCZ103490 ×4.6; *5*, 19 thoracic segments, MCZ114934 ×3.4; *6*, 19 thoracic segments, MCZ116074 ×3.1; *7*, 20 thoracic segments, NMNH475499 ×5.0; *8*, 20 thoracic segments, NMPL39840 ×3.4; *9*, 20 thoracic segments, BMNH59826.8 ×3.2.

https://doi.org/10.1666/13-142 Published online by Cambridge University Press

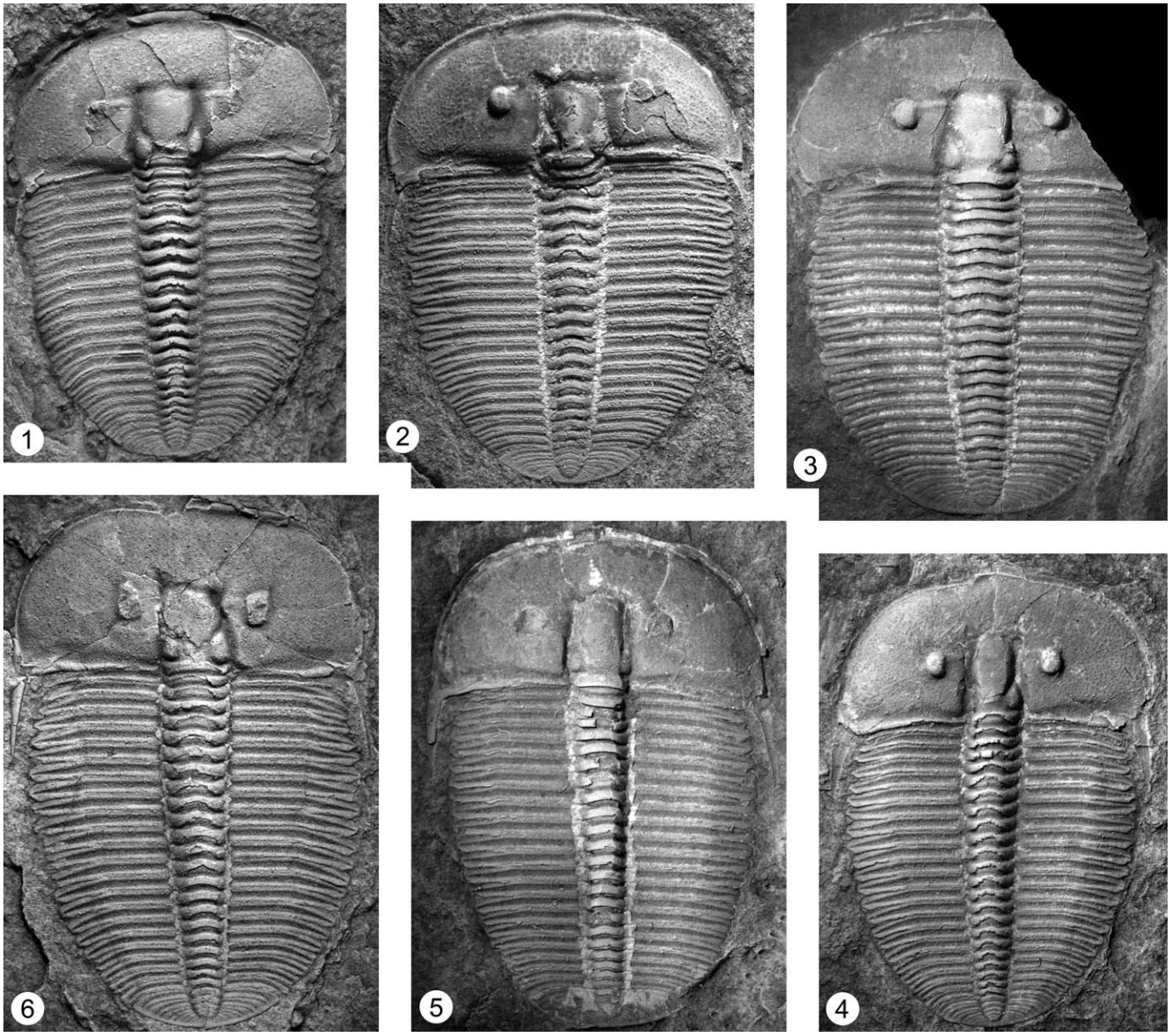

FIGURE 19—*Aulacopleura koninckii* (Barrande, 1846a) from Na Černidlech, Czech Republic; specimens coated with magnesium oxide prior to photography: *1*, 21 thoracic segments, MCZ114950 ×5.1; *2*, 21 thoracic segments, MCZ176470 ×3.8; *3*, 21 thoracic segments, NMPL39848 ×3.2; *4*, 22 thoracic segments, NMPL39850 ×3.6; *5*, 22 thoracic segments, NMPL39851 ×3.3; *6*, 22 thoracic segments, MCZ114877 ×3.2.

Middle Gill near Cautley in Cumbria County of northwestern England has questionably been designated as *Otarion* (*Aulacopleura*) *koninckii* by Thomas (1978). This author also considered *Arethusina* sp. Marr, 1913 of the Wenlockian (lower Sheinwoodian) *Cryptograptus murchisoni* Zone and *Aulocopleura* [sic] sp. Rickards, 1967 of the *C. centrifugus* Zone from the same locality to be conspecific. Since Marr (1913) did not illustrate any specimen of the taxon, and whereabouts of Rickards' specimens are unknown (Thomas, 1978, p. 29), these assessments can only be assessed when more complete material is found. Specimens questionably assigned to *Arethusina koninckii* by Reed (1904) from the Upper Balclatchie Group (Late Ordovician) of Balclatchie near Girvan, South Ayrshire, Scotland are *Paraaulacopleura reedi* (Přibyl, 1947), and the cranidial specimen has been reillustrated by Morris and Tripp (1986, pl. 3, fig. 2).

Occurrence of *A. koninckii* from the following areas is questionable due to insufficient information on the specimens: Ostratcodenkalk Formation, Wenlock, Tonhalde quarry near Lindener Mark, Gießen, Hesse State, Rhenish Massif, west-central Germany (Kegel, 1928); *Retiolites* Beds, lower Wenlock, Styggforsen and Nittsjö, Siljan, Dalarna County, central Sweden (Törnquist, 1884); upper Silurian of Montagne Noire, southern France (Bergeron, 1890); upper Silurian of Barcelona, Catalonia, Pyrenees, northeastern Spain (Hernández Sampelayo, 1942); upper Ludlow of Bou Regreg, Morocco (Lecointre, 1926).

Remarks.—Taxa that had been designated as subspecies or variants of *A. koninckii* include *Arethusina koninckii* var. *peralta* Katzer, 1895, *Aulacopleura koninckii* var. *occitanica* Chaubet, 1937, and *Aulacopleura* (*A.*) *koninckii haueri* (Frech, 1887) in Přibyl, 1947, but we consider subspecies to be unnecessary.

Arethusina koninckii var. *peralta* of Katzer (1895) has been documented as occurring with the common *A. koninckii* in the

https://doi.org/10.1666/13-142 Published online by Cambridge University Press

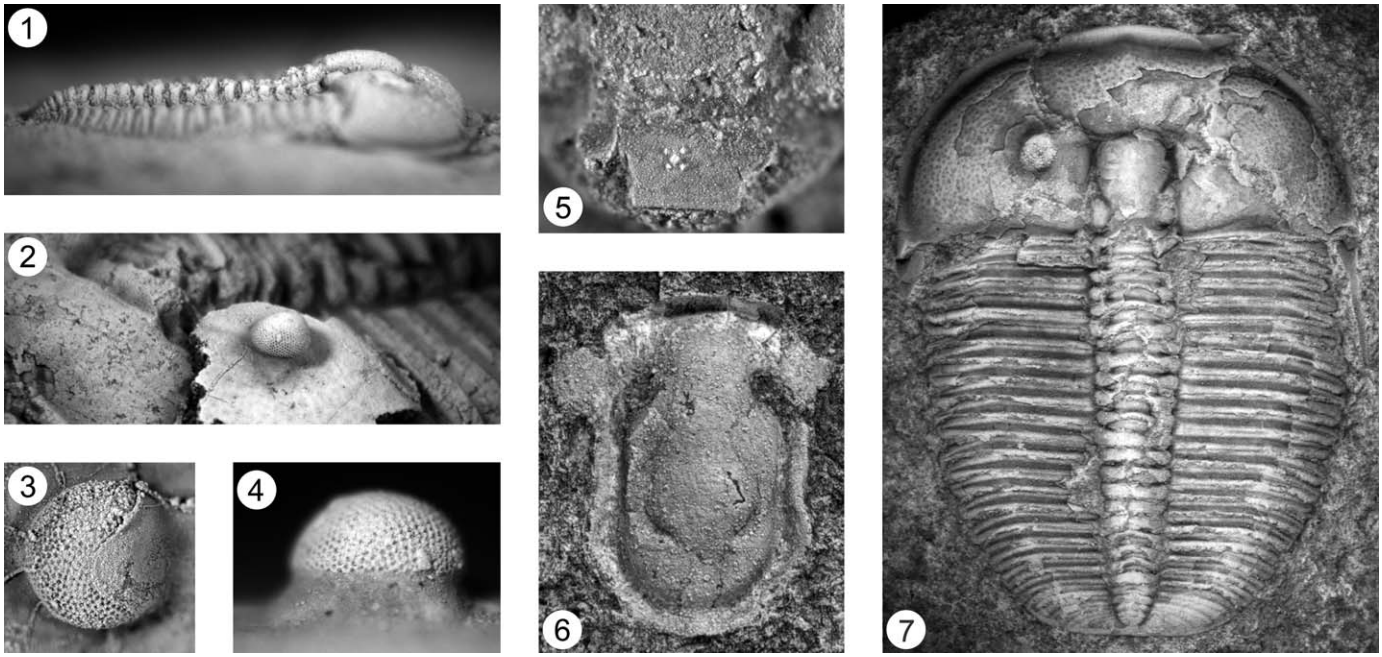

FIGURE *20—Aulacopleura koninckii* (Barrande, 1846a) from Na Černidlech and *Arethusina* Gorge, Czech Republic; specimens coated with magnesium oxide prior to photography: *1*, lateral view, NMPL39890 ×11.0; *2–4*, oblique, dorsal, and lateral views of the eye, NMPL39942A ×7.0, ×17.0, ×20.0; *5*, cephalic median organ on LO, MCZ116031 ×25.0; *6*, hypostome, MCZ116102D ×6.3; *7*, lectotype, NMPL2236 ×4.0.

gray fine-grained limestone of Barrande's bandes "Ee2" at "Kozelfelsen," and has only been figured in drawings (Katzer, 1895, pl. 1, figs. 3, 3a–3c; Prantl and Přibyl, 1950, pl. 2, figs. 1–3). The locality is now known as the Berounka Valley, Lištice, Beroun District, Czech Republic, and the Kozel limestone complex is estimated to be the Wenlock (Homerian) *P. dubius parvus* Zone (Kříž, 1992; Kříž et al., 1993). The high degree of cephalic convexity was emphasized as the principle character for this variant (Katzer, 1895, p. 9), but high relief is due to preservation in limestone which is much more resistant to compaction than shale, and so we did not consider this form to be taxonomically meaningful. Prantl and Přibyl (1950) considered this variant to belong to *A*. (*A*.) *koninckii haueri* (Frech, 1887) mainly based on its convexity of the cephalic shield and the prominent anteromedial notch in the cephalic border (Přibyl, 1947, p. 540). However, the extent of the notch is observed to be quite variable in the collection of *A. koninckii* from Na Černidlech, ranging from being absent to being quite striking (Fig. 19.4). Therefore, Katzer's specimen probably belongs within *A. koninckii*.

Aulacopleura koninckii var. *occitanica* Chaubet, 1937 was reported from the *Monograptus priodon* Zone of Roquemaillère, Montagne Noire. Its eye ridge slope backwards abaxially, and the glabella is too wide to be a species of *Aulacopleura*. It is better referred to *Paraaulacopleura*.

Frech (1887) erected the species *Arethusina haueri* for *Aulacopleura* species found from the *Orthoceras* beds of the Kok limestones in the Carnic Alps (Hertisch, 1929; Gärtner, 1930; Santel, 2001). Convexity of the cephalic shield was the main character that distinguished the species from *A. koninckii*, and Přibyl (1947) later treated the species as a subspecies of *A. koninckii*, *A*. (*A*.) *koninckii haueri*, using the anteriormedial notch on the cephalic border as the main distinguishing character. Thorough examination of the wide possible spectrum of morphology of *A. koninckii* specimens in this study sufficiently illustrates that the morphology of the Carnic Alps taxon lies within the morphological variation range seen at Na Černidlech and so we consider this taxon to be a junior synonym of *A. koninckii*.

Phylogenetic relationships within *Aulacopleura* are quite poorly resolved, but have been the subject of some phylogenetic analysis (Yuan et al., 2001, fig. 4). *Aulacopleura wulongensis* differs from *A. koninckii* in having a shorter preglabellar area, a wider anterior cranidial border, and a wider distance between the eyes. The species has 16 thoracic segments in the holaspid phase compared to the 18–22 segments of holaspid *A. koninckii*. It occurs stratigraphically lower than *A. koninckii* in the Aeronian Stage (Wang, 1989; Yuan et al., 2001) of the Llandovery of southern China.

Aulacopleura krizi differs from *A. koninckii* in having a much shorter preglabellar area, more posteriorly located eyes, and a much smaller maximum cephalic width. It occurs in the *L. convolutus* Zone to the *S. sedgwickii* Zone of upper Želkovice Formation, uppermost Aeronian, Llandovery at Hýskov near Beroun, Czech Republic (Šnajdr, 1975, 1978; Kříž, 1992). Šnajdr (1978) recorded 15 thoracic segments for what he claimed to be small holotype with a total length of 9.4 mm, but this length is within the meraspid size range for *A. koninckii,* and so we cannot be confident that this specimen was holaspid. Accordingly, the number of thoracic segments in the holaspid phase of this species is not known.

The Australian form *Aulacopleura pogsoni* differs from *A. koninckii* in having more posteriorly located eyes, and a wider (trans.) distance between the eyes. The maximum observed number of thoracic segments is 17 in forms likely to be holaspid based on size comparision with *A. koninckii*. The species occurs in the *S. turriculatus* Zone, upper part of Cotton Formation, Telychian, Llandovery (Edgecombe and Sherwin, 2001).

Aulacopleura andersoni differs from *A. koninckii* in having a shorter preglabellar area, a much narrower anterior cranidial border, larger eyes, and a much narrower maximum cephalic width. The species occurs in the *P. celloni* Zone to *P. amorphognathoides* Zone, Whittaker Formation, upper Telychian, Llandovery (Adrain and Chatterton, 1995).

https://doi.org/10.1666/13-142 Published online by Cambridge University Press

Aulacopleura soror differs from *A. koninckii* in having a slightly shorter preglabellar area, and coarse pustules most prominently on surface of the preglabellar area. The species occurs with *Plectograptus* cf. *praemacilentus* in the *T. testis* Zone, Motol Formation, lower Homerian, Wenlock in the Herinky Hill near Lištice, and at Vyskočilka of Malá Chuchle, Czech Republic (Přibyl et al., 1985).

ACKNOWLEDGMENTS

Access to the collections in Prague was kindly made available by V. Turek of the Czech National Museum, and P. Budil of the Czech Geological Survey, and we also thank them for their assistance. Material from the Museum of Comparative Zoology, Harvard University; Natural History Museum, London; National Museum of Natural History, Washington D.C.; and the American Museum of Natural History, New York was made available to us through the efforts of J. Cundiff, C. Mellish, M. Florence, and B. Hussaini respectively. We also thank G. Fusco, J. Kříž, A. Rushton, and M. Webster for discussions during this work. C. Crônier and T. Hegna provided insightful reviews. This work was funded by grant NSF EAR-0616574.

ACCESSIBILITY OF SUPPLEMENTAL DATA

Supplemental data deposited in Dryad repository: http://dx.doi.org/10.5061/dryad.4m5b5.

REFERENCES

ADRAIN, J. M. 2011. Class Trilobita Walch, 1771, p. 104–109. *In* Z.-Q. Zhang (ed.), Animal Biodiversity: An Outline of Higher-level Classification and Survey of Taxonomic Richness. Zootaxa Monograph 3148.

ADRAIN, J. M. AND B. D. E. CHATTERTON. 1993. A new rorringtoniid trilobite from the Ludlow of Artic Canada. Canadian Journal of Earth Sciences, 30: 1634–1643.

ADRAIN, J. M. AND B. D. E. CHATTERTON. 1995. Aulacopleurine trilobites from the Llandovery of northwestern Canada. Journal of Paleontology, 69:326–340.

ANGELIN, N. P. 1854. Palaeontologia Scandinavica. Pars 1: Crustacea Formations Transitionis. Fascicle 2: Palaeontologia Scandinavica. Berlingianis, Lund, 72 p.

BARRANDE, J. 1846a. Notice Préliminaire sur le Système Silurien et les Trilobites de Bohême. Hirschfield, Leipzig, 96 p.

BARRANDE, J. 1846b. Nouveaux Trilobites Supplément à la Notice Préliminaire sur le Système Silurien et les Trilobites de Bohême. Calve, Prague, 40 p.

BARRANDE, J. 1852. Système Silurien du Centre de la Bohême. I. Recherches Paléontologiques, vol. 1 (Crustacés: Trilobites). Prague and Paris, 935 p.

BERGERON, M. J. 1890. Sur la présence, dans le Languedoc, de certaines espèces de l'étage e_1 du Silurien supérieur de Bohême. Bulletin de la Société Géologique de France, Troisième Série, 18:171–174.

BRETT, C. E., J. J. ZAMBITO, B. R. HUNDA, AND E. SCHINDLER. 2012. Mid-Paleozoic trilobite lagerstätten: models of diagenetically enhanced obrution deposits. PALAIOS, 27:326–345.

CHATTERTON, B. D. E. 1980. Ontogenetic studies of middle Ordovician trilobites from the Esbataottine Formation, Mackenzie Mountains, Canada. Palaeontographica Abteilung A, 171:1–74.

CHAUBET, M.-C. 1937. Contribution á l'étude géologique du Gothlandien du versant méridional de la Montagne Noire. Travaux du Laboratoire de Géologie de la Faculté des Sciences de Montpellier, Mémoire, 1:1–224.

EDGECOMBE, G. D. AND L. SHERWIN. 2001. Early Silurian (Llandovery) trilobites from the Cotton Formation, near Forbes, New South Wales, Australia. Alcheringa, 25:87–105.

FATKA, O. AND M. MERGL. 2009. The 'microcontinent' Perunica: status and story 15 years after conception, p. 65–101. *In* M. G. Bassett (ed.), Early Palaeozoic Peri-Gondwana Terranes: New Insights from Tectonics and Biogeography. Geological Society, London, Special Publication 325.

FRECH, G. 1887. Über das Devon der Ostalpen nebst Bemerkungen über das Silur und einem paläontologischen Anhang. Zeitschrift der Deutschen Geologischen Gesellschaft, 39:659–738.

FUSCO, G., N. C. HUGHES, M. WEBSTER, AND A. MINELLI. 2004. Exploring developmental modes in a fossil arthropod: growth and trunk segmentation of the trilobite *Aulacopleura konincki*. American Naturalist, 163:167–183.

FUSCO, G., P. S. HONG, AND N. C. HUGHES. 2014. Positional specification in the segmental growth pattern of an early arthropod. Proceeding of the Royal Society, Series B, 281(1781):20133037.

GÄRTNER, H. R. 1930. Silurische und teifunterdevonische Trilobiten und Brachiopoden aus den Karnischen Alpen. Jahrbuch der Preußischen Geologischen Landesanstalt zu Berlin, 51:188–252.

HAMMER, Ø. AND D. A. T. HARPER. 2006. Paleontological Data Analysis. Blackwell Publishing, Malden, MA, 351 p.

HAWLE, I. AND A. J. C. CORDA. 1847. Prodrom einer Monographie der böhmischen Trilobiten. Abhandlungen der Königlichen böhmischen Gesellschaft der Wissenschaften, 5:1–176.

HERNÁNDEZ SAMPELAYO, P. 1942. Explicación del nuevo mapa geológico de España. Tomo II. El Sistema Siluriano. Memorias del Instituto Geológico y Minero de España, 45:1–848.

HERTISCH, F. 1929. Faunen aus dem Silur der Ostalpen. Abhandlungen der Geologischen Bundersanstalt, 23:1–183.

HORNÝ, R. AND F. BASTL. 1970. Type specimens of fossils in the National Museum, Prague. Volume 1, Trilobita. Museum of Natural History, Prague, 354 p.

HORNÝ, R., F. PRANTL, AND J. VANĚK. 1958. K otázce hranice mezi wenlockem a ludlowem v Barrandienu. Sborník Ústředního ústavu geologického, 24: 217–278.

HUGHES, N. C. 1999. Statistical and imaging methods applied to deformed fossils, p. 127–155. *In* D. A. T. Harper (ed.), Numerical Palaeobiology. John Wiley, London.

HUGHES, N. C. 2003a. Trilobite tagmosis and body patterning from morphological and developmental perspectives. Integrative and Comparative Biology, 43:185–206.

HUGHES, N. C. 2003b. Trilobite body patterning and the evolution of arthropod tagmosis. BioEssays, 25:386–395.

HUGHES, N. C. 2005. Trilobite reconstruction: building a bridge across the micro- and macroevolutionary divide. p. 139–158. *In* D. E. G. Briggs (ed.), Evolving Form and Function: Fossils and Development: Proceedings of a Symposium Honoring Adolf Seilacher for his Contributions to Paleontology, in Celebration of his 80th Birthday. Peabody Museum of Natural History, Yale Univeristy, New Haven.

HUGHES, N. C. 2007. The evolution of trilobite body patterning. Annual Reviews in Earth and Planetary Sciences, 35:401–434.

HUGHES, N. C. AND R. E. CHAPMAN. 1995. Growth and variation in the Silurian proetide trilobite *Aulacopleura konincki* and its implications for trilobite palaeobiology. Lethaia, 28:333–353.

HUGHES, N. C. AND R. E. CHAPMAN. 2001. Morphometry and phylogeny in the resolution of paleobiological problems–unlocking the evolutionary significance of an assemblage of Silurian trilobites, p. 29–54. *In* J. M. Adrain, G. D. Edgecombe, and B. S. Lieberman (eds.), Fossils, Phylogeny, and Form. Topics in Geobiology 19.

HUGHES, N. C., R. E. CHAPMAN, AND J. M. ADRAIN. 1999. The stability of thoracic segmentation in trilobites: a case study in developmental and ecological constraints. Evolution and Development, 1:24–35.

HUGHES, N. C., J. T. HAUG, AND D. WALOSZEK. 2008. Basal euarthropod development: a fossil-based perspective, p. 281–298. *In* A. Minelli and G. Fusco (eds.), Evolving Pathways: Key Themes in Evolutionary Developmental Biology. Cambridge University Press, New York.

HUGHES, N. C. AND P. A. JELL. 1992. A statistical/computer-graphic technique for assessing variation in tectonically deformed fossils and its application to Cambrian trilobites from Kashmir. Lethaia, 25:317–330.

HUGHES, N. C., J. KŘÍŽ, J. H. S. MACQUAKER, AND W. D. HUFF. 2014. The depositional environment and taphonomy of the Homerian "*Aulacopleura* shales" fossil assemblage near Loděnice, Czech Republic (Prague Basin, Perunican microcontinent). Bulletin of Geosciences, 89:219–238.

HUGHES, N. C., A. MINELLI, AND G. FUSCO. 2006. The ontogeny of trilobite segmentation: a comparative approach. Paleobiology, 32:602–627.

JELL, P. A. AND J. M. ADRAIN. 2003. Available generic names for trilobites. Memoirs of the Queensland Museum, 48:331–553.

KATZER, F. 1895. Beiträge zur Palaeontologie des älteren Palaeozoicums in Mittelböhmen. Sitzungsberichte der Königl, Böhmischen Gesellschaft der Wissenschaften, Mathematisch-naturwissenschaftliche Classe, 14:1–17.

KEGEL, W. 1928. Über obersilurische Trilobiten aus dem Harz und dem Rheinischen Schiefergebirge. Jahrbuch der Preußischen Geologischen Landesanstalt zu Berlin, 48:616–647.

KŘÍŽ, J. 1992. Silurian Field Excursions: Prague Basin (Barrandian), Bohemia. National Museum of Wales, Geological Series, 13, 111 p.

KŘÍŽ, J. 1999. Silurian and lowermost Devonian bivalves of Bohemian type from the Carnic Alps. Abhandlungen der Geologischen Bundesanstalt, 56: 259–316.

KŘÍŽ, J., P. DUFKA, H. JAEGER, AND H. P. SCHÖNLAUB. 1993. The Wenlock/Ludlow boundary in the Prague Basin (Bohemia). Jahrbuch der Geologischen Bundesanstalt, 136:809–839.

LECOINTRE, G. 1926. Recherches géologiques dans la Meseta Marocaine. Mémoires de la Société des sciences naturelles du Maroc, 14:1–151.

LU, Y.-H. 1975. Ordovician trilobite faunas of central and southwestern China. Palaeontologia Sinica, New Series B, 11:1–463.

LUDVIGSEN, R. AND R. P. TRIPP. 1990. Silurian trilobites from the northern Yukon Territory. Royal Ontario Museum, Life Sciences Contributions, 153: 1–59.

MARR, J. E. 1913. The lower Palaeozoic rocks of the Cautley District (Yorkshire). Quarterly Journal of the Geological Society of London, 69:1–18.

MORRIS, S. F. AND R. P. TRIPP. 1986. Lectotype selections for Ordovician trilobites from the Girvan District, Strathclyde. Bulletin of the British Museum (Natural History) Geology, 40:161–196.

OWENS, R. M. AND W. HAMMANN. 1990. Proetide trilobites from the Cystoid Limestone (Ashgill) of NW Spain, and the supragenic classification of related forms. Paläontologische Zeitschrift, 64:221–244.

POULSEN, C. 1934. The Silurian faunas of North Greenland, 1. The fauna of the Cape Schuchert Formation. Meddelelser om Grønland, 72:1–46.

PRANTL, F. AND A. PŘIBYL. 1950. Revise čeledi Otarionidae R. a E. Richter z českého siluru a devonu (Trilobitae). Zvláštní ostisk ve Sborníku státního geologického ústavu Československé republiky, 17:353–512.

PŘIBYL, A. 1947. *Aulacopleura* and the Otarionidae. Journal of Paleontology, 21:537–545.

PŘIBYL, A. AND J. VANĚK. 1981. Studie zur Morphologie und Phylogenie der Familie Otarionidae R. U. E. Richter, 1926 (Trilobita). Palaeontographica Abteilung A, 173:160–208.

PŘIBYL, A., J. VANĚK, AND F. HÖRBINGER. 1985. New taxa of Proetacea (Trilobita) from the Silurian and Devonian of Bohemia. Časopis pro mineralogii a geologii, 30:237–251.

REED, F. R. C. 1904. The Lower Palaeozoic Trilobites of the Girvan District, Ayrshire. Part II. Palaeontological Society Monograph, 47 p.

RICKARDS, R. B. 1967. The Wenlock and Ludlow succession in the Howgill Fells (north-west Yorkshire and Westmoreland). Quarterly Journal of the Geological Soceity of London, 69:1–18.

SANTEL, W. 2001. Trilobiten aus dem Silur der Karnischen Alpen/Österreich Teil I. Palaeontographica Abteilung A, 262:87–191.

SCHINDEWOLF, O. H. 1924. Vorläufige Übersicht über die Obersilur-Fauna des "Elbersreuther Orthoceratitekalkes," 1. Allgemeine Vorbemerkungen und Trilobitenfauna. Senckenbergiana, 6:187–221.

ŠNAJDR, M. 1975. New Trilobita from the Llandovery at Hýskov in the Beroun area, central Bohemia. Věstník Ústředního ústavu geologického, 50:311–316.

ŠNAJDR, M. 1978. The Llandoverian trilobites from Hýskov (Barrandian area). Sborník geologických věd, Paleontologie, 21:7–45.

ŠNAJDR, M. 1990. Bohemian Trilobites. Geological Survey, Prague, 265 p.

ŠTORCH, P. 2006. Facies development, depositional settings and sequence stratigraphy across the Ordovician–Silurian boundary; a new perspective from the Barrandian area of the Czech Republic. Geological Journal, 41: 163–192.

THOMAS, A. T. 1978. British Wenlock Trilobites Part 1. Palaeontographical Society Monographs, 552, 56 p.

THOMAS, A. T. AND R. M. OWENS. 1978. A review of the trilobite family Aulacopleuridae. Palaeontology, 21:65–81.

TOMCZYKOWA, E. 1957. Trylobity z łupków graptolitowych wenloku i dolnego ludlowu Gór Świętokrzyskich. Biuletyn Instytutu Geologicznego, 122:83–114.

TÖRNQUIST, S. L. 1884. Undersökningar öfver Siljansomradets trilobitfauna. Sveriges Geologiska Undersökning (Serie C), 66:1–101.

WANG, Q.-Z. 1989. Early Silurian trilobites from Wulong, southeastern Sichuan (China). Journal of Hebei College of Geology, 12:422–440.

WEBSTER, M. 2011. The structure of cranidial shape variation in three early ptychoparioid trilobite species from the Dyeran–Delamaran (traditional "lower–middle" Cambrian) boundary interval of Nevada, U.S.A. Journal of Paleontology, 85:179–225.

YUAN, W.-W., L.-Z. LI, Z.-Y. ZHOU, AND C.-S. ZHANG. 2001. Ontogeny of the Silurian trilobite *Aulacopleura* (*Aulacopleura*) *wulongensis* Wang of western Hubei and its implications for the phylogeny of the Aulacopleurinae. Acta Palaeontologica Sinica, 40:388–398.

ZELDITCH, M. L., D. L. SWIDERSKI, H. D. SHEETS, AND W. L. FINK. 2004. Geometric Morphometrics for Biologists: A Primer. Academic Press, San Diego, 443 p.

ACCEPTED 29 MARCH 2014